

A STOCHASTIC SPATIAL MODEL FOR THE CONSUMPTION OF ORGANIC
FOREST SOILS IN A SMOLDERING GROUND FIRE

HUMBOLDT STATE UNIVERSITY

By

Benjamin Victor Holt

A Thesis

Presented to

The Faculty of Humboldt State University

In Partial Fulfillment

Of the Requirements for the Degree

Master of Science

In Environmental Systems: Mathematical Modeling

May 2008

A STOCHASTIC SPATIAL MODEL FOR THE CONSUMPTION OF ORGANIC
FOREST SOILS IN A SMOLDERING GROUND FIRE

HUMBOLDT STATE UNIVERSITY

By

Benjamin Victor Holt

Approved by the Master's Thesis Committee:

Dr. Elizabeth Burroughs, Major Professor Date

Dr. Chris Dugaw, Committee Member Date

Dr. J. Morgan Varner, Committee Member Date

Dr. Sharon Brown, Graduate Coordinator Date

Dr. Chris A. Hopper, Interim Dean Date
Research, Graduate Studies & International Programs

ABSTRACT

A STOCHASTIC SPATIAL MODEL FOR THE CONSUMPTION OF ORGANIC FOREST SOILS IN A SMOLDERING GROUND FIRE

Benjamin Victor Holt

A spatial model for the consumption of organic forest soil (duff) by smoldering combustion is developed. Smoldering ground fires have an enormous impact upon the ecology and management practice of forest lands throughout the temperate zone. It is the goal of this effort to predict, and hence better understand, observed spatial patterns in duff consumption. Models of duff consumption are often empirically derived and consequently too specific to the site of study. Additionally, models of duff consumption based upon models of smoldering combustion are difficult to use and can yield questionable results since few, if any, models of smoldering combustion are created specifically for duff. This effort seeks to circumvent such shortcomings by creating a general duff consumption model that requires a small number of user-determined parameters that are easily estimated from field samples. These parameters include organic bulk density, moisture content, mineral content, and duff depth. The fuel-bed is modeled by a two-dimensional stochastically updated cellular automaton. Model output compares favorably to empirical and field studies concerning spatial aspects of duff consumption. Modifications to the model are proposed that would advance understanding of the ecological impact of duff consumption.

ACKNOWLEDGEMENTS

To my committee, Dr. Elizabeth Burroughs, Dr. Christopher Dugaw, and Dr. J. Morgan Varner, I extend my warmest thanks for their wisdom concerning all aspects of this work. Their thoughtful feedback and criticism have greatly improved the quality and focus of this effort. Their multiple, thorough, and detailed readings of the drafts preceding the final form have yielded a product far better than I could have achieved working alone.

I thank Beth for her patient and skillful guidance as my advisor. Her direction and advice concerning modeling and numerical issues was absolutely essential to this work. I could not have asked for a more pleasant and gifted person to direct my efforts.

I thank Chris for his ideas and feedback in every stage of model development. Also, the skills acquired by his excellent instruction in the several courses I have taken from him have proven to be of tremendous value in my modeling efforts. Additionally, I am forever in his debt for requiring me to learn \LaTeX early in my program here.

I thank Morgan for helping me get started on this project by pointing me in the right direction, giving me papers to read, listening to ideas, and offering suggestions. I also thank Morgan for taking the time to help me acquire field experience that was invaluable to gaining a rudimentary intuition concerning forest duff, and hence, to the completion of this work.

Special thanks to Dr. Gaylon S. Campbell for correspondence that helped greatly with the implementation of the model.

Thanks to all the mathematics faculty at Humboldt State University who have been an absolute joy to learn from: Dr. Charlie Biles, Dr. Sharon Brown, Dr. Phyllis Chinn, Dr. Tyler Evans, Dr. Walden Freedman, Dr. Jeff Haag, Dr. Bob Hunt, Dr. Diane Johnson, Dr. Dale Oliver, Dr. Ken Owens, Dr. Mark Rizzardi, and Dr. Ken Yanosko.

For laying the mathematical foundation that has served me so well these many years, I would like to thank Maryl Landess, Laurel Grindy, and Virginia Gray of Columbia College. Special thanks to Dr. Dennis Albers of Columbia College for an extraordinarily solid introduction to physics and modeling.

Thanks to all of my friends, family and teachers who have encouraged my interests and sustained me throughout the years: Gabriel DeHerrera, Paul and Theresa Baumbay, Renée and Jim Compel, Michael Fijman, Maria Cristina Long, Trinidad and Pennelys Goodshield, L. Maxwell Shere, Don Pierazzi, Emily Hobelmann, Michelle Moreno, Iris Gray, Dan Kanewske, Francis Chan, Jennifer Sorkin, Scott Cresswell, Carolyn Yawn, Jeremy Cotton, Darrell Ross, Steve Walker, Paul Cunningham, Cliff Crawford, Sigrid Andersen, Robert Hohn, and Paul Nixon.

Special thanks to Raymond and Patricia Harrelson and the entire Harrelson family for their love and support at a time when I needed it most.

For her love and support in all of my endeavors, I thank my mother, Pauline Hamilton-Werning. To her, and to the memory of Dr. Theodore Werning, I lovingly dedicate this work.

TABLE OF CONTENTS

ABSTRACT	iii
ACKNOWLEDGEMENTS	iv
TABLE OF CONTENTS	vi
LIST OF FIGURES	vii
NOMENCLATURE	xi
INTRODUCTION	1
LITERATURE REVIEW	6
MODEL	12
The Fuel Bed	12
Initialization	16
Temperature and Moisture Dynamics	17
Update Rules	22
Combustion State	22
Volumetric Moisture Content	29
Gravimetric Moisture Content	31
Temperature	32
Implementation	37
RESULTS AND DISCUSSION	38
Overall Model Behavior	38
Spatial Patterns	38
The Drying Front	39
Comparison of Model Behavior to Other Studies	52
Observed Spatial Patterns	52
The Limits of Smoldering Combustion	54
Smolder Velocity	56
The Effect of Depth	59
MODIFICATIONS AND FUTURE WORK	63
CONCLUSIONS	71
BIBLIOGRAPHY	72

LIST OF FIGURES

Figure		Page
1	A vertical cross-section of forest soil with pronounced litter, fermentation, humus, and mineral soil horizons (photograph courtesy of J.M. Varner). . . .	2
2	Overall model structure for predicting the spatial pattern of forest floor duff consumption.	13
3	Cell (i, j) and its four nearest neighbors.	14
4	Three stage model of the combustion process in forest duff.	15
5	The uninhibited smoldering front (with the initial burn edge on the left) when 80% of cells have become active.	25
6	The average distance from the initial burn edge (left) versus time (blue). The slope of the regression line (green) is taken to be the average smolder velocity. The lower graph (50-150 hours) is a magnification of the upper graph (0-400 hours).	26
7	The evolution of a simulated smoldering front showing the spatial patterns that emerge for dry duff (20% GMC) with center ignition using regression coefficients for spruce/pine duff. $\mu_\gamma = 0.2$ kg/kg, $\mu_\rho = 116$ kg/m ³ , $\mu_\alpha = 0.307$ kg/kg, and $\mu_\tau = 0.15$ m.	40
8	The evolution of a simulated smoldering front showing the spatial patterns that emerge for moist duff (105% GMC) with center ignition using regression coefficients for spruce/pine duff. $\mu_\gamma = 1.05$ kg/kg, $\mu_\rho = 116$ kg/m ³ , $\mu_\alpha = 0.307$ kg/kg, and $\mu_\tau = 0.15$ m.	41
9	The evolution of a simulated smoldering front showing the spatial patterns that emerge for very moist duff (110% GMC) with center ignition using regression coefficients for spruce/pine duff. $\mu_\gamma = 1.1$ kg/kg, $\mu_\rho = 116$ kg/m ³ , $\mu_\alpha = 0.307$ kg/kg, and $\mu_\tau = 0.15$ m.	42
10	The evolution of a simulated smoldering front showing the spatial patterns that emerge for dry duff (20% GMC) with left edge ignition using regression coefficients for spruce/pine duff. $\mu_\gamma = 0.2$ kg/kg, $\mu_\rho = 116$ kg/m ³ , $\mu_\alpha = 0.307$ kg/kg, and $\mu_\tau = 0.15$ m.	43

11	The evolution of a simulated smoldering front showing the spatial patterns that emerge for moist duff (105% GMC) with left edge ignition using regression coefficients for spruce/pine duff. $\mu_\gamma = 1.05 \text{ kg/kg}$, $\mu_\rho = 116 \text{ kg/m}^3$, $\mu_\alpha = 0.307 \text{ kg/kg}$, and $\mu_\tau = 0.15 \text{ m}$	44
12	The evolution of a simulated smoldering front showing the spatial patterns that emerge for very moist duff (110% GMC) with left edge ignition using regression coefficients for spruce/pine duff. $\mu_\gamma = 1.1 \text{ kg/kg}$, $\mu_\rho = 116 \text{ kg/m}^3$, $\mu_\alpha = 0.307 \text{ kg/kg}$, and $\mu_\tau = 0.15 \text{ m}$	45
13	The resulting burn pattern for six consecutive model runs with moist duff (105% GMC) allowing the simulation to proceed until all combustion ceased. Ignition was initiated at the center. The initial uniform duff conditions were $\mu_\gamma = 1.05 \text{ kg/kg}$, $\mu_\rho = 116 \text{ kg/m}^3$, $\mu_\alpha = 0.307 \text{ kg/kg}$, and $\mu_\tau = 0.15 \text{ m}$	46
14	The resulting burn pattern for six consecutive model runs with very moist duff (110% GMC) allowing the simulation to proceed until all combustion ceased. Ignition was initiated in the center. The initial duff conditions were $\mu_\gamma = 1.1 \text{ kg/kg}$, $\mu_\rho = 116 \text{ kg/m}^3$, $\mu_\alpha = 0.307 \text{ kg/kg}$, and $\mu_\tau = 0.15 \text{ m}$	47
15	The resulting burn pattern for six consecutive model runs with moist duff allowing (105% GMC) the simulation to proceed until all combustion ceased. Ignition was initiated at the left edge. The initial duff conditions were $\mu_\gamma = 1.05 \text{ kg/kg}$, $\mu_\rho = 116 \text{ kg/m}^3$, $\mu_\alpha = 0.307 \text{ kg/kg}$, and $\mu_\tau = 0.15 \text{ m}$	48
16	The resulting burn pattern for six consecutive model runs with very moist duff (110% GMC) allowing the simulation to proceed until all combustion ceased. Ignition was initiated at the left edge. The initial duff conditions were $\mu_\gamma = 1.1 \text{ kg/kg}$, $\mu_\rho = 116 \text{ kg/m}^3$, $\mu_\alpha = 0.307 \text{ kg/kg}$, and $\mu_\tau = 0.15 \text{ m}$	49
17	Histogram for the area (in square meters) of simulated burned patch sizes near the limits of smoldering combustion (very moist duff, 110% GMC) for 2400 trials with ignition initiated at the center of the lattice. $\mu_\gamma = 1.1 \text{ kg/kg}$, $\mu_\rho = 116 \text{ kg/m}^3$, $\mu_\alpha = 0.307 \text{ kg/kg}$, and $\mu_\tau = 0.15 \text{ m}$	50
18	A model run in progress displaying also the heat and moisture dynamics. The predicted drying front is seen in the bottom left graph displaying moisture content versus space. $\mu_\gamma = 0.7 \text{ kg/kg}$, $\mu_\rho = 116 \text{ kg/m}^3$, $\mu_\alpha = 0.487 \text{ kg/kg}$, and $\mu_\tau = 0.15 \text{ m}$	51

19	Smoldering duff in an aspen dominated stand during a prescribed burn. Ecosystem Management Emulating Natural Disturbance Project, North-western Alberta, Canada (photograph by David P. Shorthouse, University of Alberta, Bugwood.org).	52
20	Close up of smoldering duff with clearly defined smoldering boundary (photograph courtesy of J.M. Varner).	53
21	Thermal infrared image of duff smoldering at the base of a tree stem (image courtesy of J.M. Varner).	54
22	Mikron IR Camera image of smoldering duff (source: USFS-Missoula Montana Fire Science Lab).	55
23	The proportion (denoted by color scale) of a simulated 10m by 10m patch of spruce/pine duff consumed by smoldering combustion expressed in terms of inorganic and moisture ratio. Each point represents the result of a single trial. $\mu_\rho = 116 \text{ kg/m}^3$, $\mu_\tau = 0.15 \text{ m}$	55
24	The proportion of a simulated 10m by 10m patch of white spruce duff consumed by smoldering combustion expressed in terms of inorganic and moisture ratio. Each point represents the result of a single trial. $\mu_\rho = 116 \text{ kg/m}^3$, $\mu_\tau = 0.15 \text{ m}$	57
25	A comparison of simulated smolder velocities (top) for spruce/pine duff, $\mu_\rho = 116 \text{ kg/m}^3$, $\mu_\tau = 0.15 \text{ m}$, and smolder velocities predicted by the empirical model (bottom) of Frandsen (1991) for peat with the same bulk density. Each point of the simulated smolder velocity graph represents the average of forty trials.	58
26	The percentage of a simulated 10m by 10m patch of spruce/pine duff consumed completely by smoldering combustion expressed in terms of depth and volumetric moisture content. Each point represents the average of five trials. $\mu_\rho = 116 \text{ kg/m}^3$, $\mu_\alpha = 0.307 \text{ kg/kg}$	61
27	The percentage of a simulated 10m by 10m patch of spruce/pine duff consumed completely by smoldering combustion expressed in terms of depth and volumetric moisture content. Each point represents the average of five trials. $\mu_\rho = 67.2 \text{ kg/m}^3$ and $\mu_\alpha = 0.307 \text{ kg/kg}$ for a simulated dry bulk density of $\mu_\delta = 97 \text{ kg/m}^3$ used by Miyanishi and Johnson (2002).	62

28	A plot of moisture-depth combinations that result in successful <i>simulated</i> smoldering propagation in spruce/pine duff where success is defined to be an average smolder distance greater than 1 meter. Red denotes successful propagation and blue represents failed propagation. Each moisture-depth combination represents 1 trial. $\mu_\rho = 67.2 \text{ kg/m}^3$ and $\mu_\alpha = 0.307 \text{ kg/kg}$ for a simulated dry bulk density of $\mu_\delta = 97 \text{ kg/m}^3$ used by Miyanishi and Johnson (2002).	62
29	A modification to the model that includes stand structure to predict tree mortality. Stand characteristics and duff conditions would be stochastically initialized with duff characteristics varying jointly with crown cover and distance from stem. Repeated simulation would estimate of tree mortality caused by exposure to smoldering duff.	64
30	A modification to the model where the lattice of cells represents a vertical cross-section of duff instead of a horizontal layer. Repeated simulation would estimate duff depth reduction.	65
31	Output from the modified model after 8 simulated days where duff depth is allowed to decrease according to duff conditions. The graph on the left represents duff depth reduction for dry conditions (20% GMC) and the graph on the right represents duff depth reduction for very moist conditions (110% GMC). Both simulations used an initial uniform depth of 0.1 m with ignition initiated in the center. Regression coefficients for spruce/pine duff were used. $\Lambda_d = \Lambda = 0.05$	66

NOMENCLATURE

Primary Duff Characteristics

- β , combustion state (unburned, burning, and burned)
- γ , gravimetric moisture content ($\frac{\text{kg}}{\text{kg}}$)
- ρ , organic bulk density ($\frac{\text{kg}}{\text{m}^3}$)
- α , ash (percent inorganic material) ($\frac{\text{kg}}{\text{kg}}$)
- τ , thickness of duff layer (m)
- θ , volumetric moisture content ($\frac{\text{m}^3}{\text{m}^3}$)
- δ , dry bulk density ($\frac{\text{kg}}{\text{m}^3}$)
- π , porosity ($\frac{\text{m}^3}{\text{m}^3}$)

Spatial, Temporal, and Lattice Variables

- Δt , time elapsed between each time-step (hr)
- $\Delta x, \Delta y$, horizontal and vertical spacing between cells (m)
- Λ , uninhibited average linear smolder velocity ($\frac{\text{m}}{\text{hr}}$) (taken to be 0.05)
- χ , scaling parameter for desired linear smolder velocity on the lattice
- ϑ , proportionality constant for mean burn time (taken to be 2.9)
- Θ , exponentially distributed burn time of a cell with mean $\vartheta \frac{\Delta x}{\Lambda}$
- E , indicates when at least one of a cell's four nearest neighbors are burning

User Determined Parameters

- B_0, B_1, B_2, B_3 , parameters for spread probability particular to duff type
- μ_ρ , mean organic bulk density ($\frac{\text{kg}}{\text{m}^3}$)
- μ_α , mean ash content ($\frac{\text{kg}}{\text{kg}}$)
- μ_γ , mean gravimetric moisture content ($\frac{\text{kg}}{\text{kg}}$)
- μ_τ , mean thickness of the duff layer (m)

Thermal and Moisture Transport Quantities

T ,	duff temperature (K)
θ ,	volumetric moisture content ($\frac{\text{m}^3}{\text{m}^3}$)
C ,	volumetric heat capacity of the duff ($\frac{\text{J}}{\text{m}^3\text{K}}$)
K ,	thermal conductivity of the duff ($\frac{\text{J}}{\text{m hr K}}$)
V ,	vapor conductivity of the duff ($\frac{\text{kg}}{\text{m hr Pa}}$)
H ,	latent heat of vaporization of water ($\frac{\text{J}}{\text{kg}}$)
p ,	partial pressure of water vapor in the duff (Pa)
C_w, C_a, C_m, C_o ,	volumetric heat capacity of duff constituents ($\frac{\text{J}}{\text{m}^3\text{K}}$)
c_w, c_a, c_m, c_o ,	specific heat capacity of each duff constituent ($\frac{\text{J}}{\text{kg K}}$)
$\lambda_w, \lambda_a, \lambda_m, \lambda_o$,	thermal conductivities of duff constituents ($\frac{\text{J}}{\text{m hr K}}$)
d_w, d_a, d_m, d_o ,	particle densities of each duff constituent ($\frac{\text{kg}}{\text{m}^3}$)
$\phi_w (= \theta), \phi_a, \phi_m, \phi_o$,	volumetric fractions of duff constituents ($\frac{\text{m}^3}{\text{m}^3}$)
k_w, k_a, k_m, k_o ,	weighting factors of each duff constituent
g_a, g_m ,	shape factors of duff constituents (taken to be 0.33 and 0.1)
P ,	saturation vapor pressure of water (Pa)
h ,	relative humidity ($\frac{\text{Pa}}{\text{Pa}}$)
ψ ,	water potential ($\frac{\text{J}}{\text{kg}}$)
D_v ,	diffusivity of water vapor in air ($\frac{\text{m}^2}{\text{hr}}$)
D_a ,	molar density of air ($\frac{\text{mol}}{\text{m}^3}$)
ξ ,	tortuosity correction (taken to be 0.66)
η ,	vapor flow enhancement factor (taken to be 1)
ζ ,	parameter reducing energy flux due to vapor flux (taken to be 0.018)

Other Model Parameters

- κ_c , convective cooling constant of the duff ($\frac{1}{\text{hr}}$) (taken to be 0.1)
- T_a , ambient temperature (K) (taken to be 293.15 K, or 20°C)
- P_a , ambient pressure (Pa) (taken to be standard pressure, 101325 Pa)
- T_c , combustion temperature of smoldering duff (K) (taken to be 673.15 K, or 400°C)
- θ_{min} , minimum VMC ($\frac{\text{m}^3}{\text{m}^3}$) (taken to be 0.01)
- $\varepsilon_1, \varepsilon_2$, efficiency parameters (respectively taken to be 9 and 150)

Constants

- M_w , molecular weight of water, 0.018 $\frac{\text{kg}}{\text{mol}}$
- R , universal gas constant, 8.314 $\frac{\text{mol}}{\text{K}}$
- P_0 , standard pressure, 101325 Pa
- T_0 , standard temperature, 273.15 K
- D_{v0} , diffusivity of water in air at standard temperature and pressure, 0.0763 $\frac{\text{m}^2}{\text{hr}}$
- D_{a0} , molar density of air at standard temperature and pressure, 44.65 $\frac{\text{mol}}{\text{m}^3}$

Abbreviations

- GMC, gravimetric moisture content
- VMC, volumetric moisture content

INTRODUCTION

Forest floor soils, especially those in regions in which fire suppression has long been practiced, are composed of several distinct layers, or *horizons* (Miyanishi, 2001) (Figure 1). The topmost horizon, commonly referred to as litter, is composed of organic materials that have not yet begun the process of decomposition. Litter includes materials that fall from trees and plants, such as fallen branches and senesced foliage. Below the litter is the fermentation horizon in which decomposition begins. The materials that compose the fermentation horizon are still recognizable as leaves, needles, twigs, and other organic debris found on the forest floor. Below the fermentation horizon is the humus horizon, which consists of these materials decomposed beyond recognition, and underneath the humus horizon is the mineral soil horizon which is low in organic content (less than 25 percent organic material). The fermentation and humus horizons together constitute what is known as the “duff layer” (Miyanishi, 2001).

Duff is largely composed of three materials: cellulose, hemicellulose, and lignin (Miyanishi, 2001). Other materials include volatiles and mineral constituents. Due to high organic content, unsaturated duff is capable of combustion. High lignin to cellulose ratios in duff inhibit the rate of production of volatile gasses necessary for sustaining flaming combustion (Miyanishi, 2001). Additionally, small particle sizes and packing ratios (the volume fraction occupied by the fuel) greater than ten percent mean that duff is consumed by smoldering combustion (Frandsen, 1991). Miyanishi (2001), however, notes that under very dry conditions thin duff layers or the upper horizons of deep duff can be consumed by a flaming front.

Ignition of the duff layer may occur either by direct contact with flaming litter or with organic debris that exhibits extended flaming combustion, particularly fallen branches and



Figure 1: A vertical cross-section of forest soil with pronounced litter, fermentation, humus, and mineral soil horizons (photograph courtesy of J.M. Varner).

pine cones (Frandsen, 1991; Varner, 2005). When ignition occurs, the duff smolders down to the mineral soil leaving it exposed, resulting in a slow, outwardly propagating smoldering perimeter, exposing more mineral soil as it moves (Frandsen, 1991; Miyanishi, 2001). The process stops when the smoldering front reaches conditions not suited to smoldering combustion: high moisture content and/or high inorganic content. If the heat generated by smoldering does not exceed the latent heat of vaporization required to drive the moisture from the duff, smoldering cannot continue (Frandsen, 1991). Also, inorganic material does not burn and only absorbs heat energy. Hence, inorganic content is also a limiting factor in the smoldering process of forest duff (Frandsen, 1991) and explains why the mineral soil is not consumed. The above processes reveal why moisture and mineral content are good predictors for the behavior of smoldering combustion in duff. Other predictors include the bulk density of organic material in the duff and duff thickness (Frandsen, 1997; Miyanishi and Johnson, 2002).

Duff consumption is of great interest to foresters and ecologists since it exerts a large influence over post-fire forest ecology. Seedlings establishing on litter and duff experience a significantly higher mortality rate than those establishing on mineral soil since the mineral soil does not dry out as quickly as duff (Miyanishi, 2001). Thus, the more duff consumed in a fire, the more suitable area that is available upon which seedlings may establish. Smoldering duff kills organisms living in the soil, either by direct consumption or by heating the mineral soil to lethal temperatures. These organisms include seeds, fungus, shrubs, trees, and bacteria. Duff also contains a wealth of nutrients so that the consumption of the duff layer plays a large role in the recycling and redistribution of these nutrients (Miyanishi, 2001).

Duff consumption is an important issue concerning both wildfires and prescribed burning. Duff may smolder long after a fire front has passed, causing secondary flaming com-

bustion in other types of fuels leading to secondary fire fronts (Frandsen, 1991). The decision to proceed with a prescribed burn is determined in part by how much duff is likely to be consumed. It is desirable that some duff be consumed since prescribed burning is a means of reducing fuel load, of which forest floor duff is a sizable component (Hille and Stephens (2005) observed an approximate fuel load percentage of 64% duff by mass). In hilly terrain it is important that some duff remain to prevent mineral soil erosion. Duff moisture is a key factor in determining how much duff is consumed. The amount of duff consumed decreases with increasing moisture. Prescribed burns in excessively moist conditions do not yield the desired reduction in fuels. However, drier burns may cause the complete consumption of the duff layer, leading to excessive tree mortality and mineral soil erosion. Great care should be taken when planning a prescribed burn near human population centers since smoke produced by smoldering combustion of duff is more noxious and polluting than that produced by flaming combustion (McMahon et al., 1980; Varner et al., 2005). Smoldering duff can be responsible for more than 50% of the smoke and pollutants produced by a forest fire (Frandsen, 1991).

Smoldering duff plays a crucial role in the reintroduction of fire to regions in which fire suppression has long been practiced. Prolonged fire suppression allows duff to accumulate that would otherwise be consumed in the low intensity fires that were historically frequent. These accumulations exhibit a profound impact on ecosystems, interfering with the recycling of nutrients and the establishment of plant and tree species. However, reintroducing fire to these ecosystems can be problematic. Duff accumulations at the base of trees may smolder at high temperatures (Figure 21) for many hours leading to excessive tree mortality, defeating the purpose of fire-reintroduction (Ryan and Frandsen, 1991; Varner et al., 2005). The mineral soil can reach temperatures in excess of 300°C (with peak temperatures of 600°C) as a result of duff consumption (Frandsen, 1991).

The objective of this effort is to develop a model to serve as a starting point for describing the spread of a smoldering ground fire that is useful, adaptable, easy to utilize, and is spatially and temporally accurate. Miyanishi (2001) notes that duff consumption models are often too specific to a given site or are based upon rather simplistic assumptions about the physical and chemical structure of organic soil as a fuel. The model proposed here addresses both shortcomings. The model is versatile in that it takes soil data for an arbitrary region as input. The data involve few key parameters to facilitate ease of use. To this end, these parameters are easy to measure. For the model presented here, these parameters include those most commonly identified in the literature as driving the process of smoldering combustion of forest soils. The versatility of the model is not limited to the reasons listed above. The model may be easily modified or integrated into other models to address other important questions concerning duff consumption, such as more general models for predicting tree mortality and reduction of duff depth. This work also acknowledges the complexity of duff as a fuel by modeling these extraordinarily complex structures and processes as a stochastic process rather than a deterministic one. Stochastic models of duff consumption by smoldering combustion may very well represent a new paradigm in the modeling of such fuels.

LITERATURE REVIEW

Duff consumption is governed by four primary soil characteristics: organic bulk density, moisture content, inorganic content, and duff depth (Frandsen, 1987; Miyanishi, 2001). Smoldering combustion of materials such as polymer foams, sawdust, and tobacco, have been studied both empirically and by modeling the combustion process (Bradbury et al., 1979; Ohlemiller, 2002). Studies that specifically seek to understand duff consumption (Frandsen, 1991, 1997, 1998) often use peat as the material of study since peat has a high organic content and is structurally similar to forest duff (Miyanishi, 2001). Frandsen (1991) statistically models the mass consumed per unit time in terms of the organic bulk density, inorganic content, and moisture content. Another study by Frandsen (1998) models heat flow from peat in terms of the mass ratios of moisture and inorganic content. A particularly useful result by Frandsen (1997) predicts the probability that a sample of organic soil will smolder in terms of its organic bulk density, moisture content, and percent inorganic content using a binary logistic regression model on burn/no burn data. The regression coefficients for each type of representative soil are given. The work of Frandsen (1997) is both unusual and remarkable in that most studies are either specific to a given site or to a particular fuel type. Other empirical studies are reviewed by Miyanishi (2001). Process-based models for pyrolysis of cellulosic materials (Bradbury et al., 1979) and smoldering propagation cited by Miyanishi (2001) and Ohlemiller (2002) represent a large body of literature devoted to a complex process. Often the predictive power of these process-based smoldering models is limited to a narrow range of conditions or fuel types. Furthermore, few, if any, process-based models of smoldering combustion are devoted to the consumption of forest duff (Miyanishi, 2001). The advantage to the empirical results of Frandsen are that they specifically seek to understand the process of duff consumption. Also, given the sheer

complexity of smoldering processes, reducing them to a statement involving probabilities as done by Frandsen (1997) is an appealing alternative to trying to account for every detail.

Other studies explicitly seek to understand spatial patterns in duff consumption. Frandsen (1991) translates the mass consumption rate of peat into a statistical model to estimate the smolder velocity of peat. Miyanishi and Johnson (2002) studied pre-fire and post-fire duff characteristics in two locations. Among these characteristics are pre- and post-burn duff depth distributions and the distribution of burned patch sizes. In addition to field study, Miyanishi and Johnson (2002) also present laboratory results concerning how duff depth influences the limits of smoldering combustion in peat. Hille and Stephens (2005) show that duff depth and the extent of duff depth reduction is related to the distance from tree crown perimeters. Since tree crowns intercept moisture, it is expected for moist duff that still favors smoldering combustion that duff depth reduction decreases with increasing distance from tree stems. Consequently, Hille and Stephens (2005) indirectly relate duff depth reduction to pre-burn duff moisture. The pre- and post-burn data collected by Hille and Stephens (2005) is used to formulate a statement of the probability that duff remains as a function of the distance from tree stems. As expected, the probability of incomplete consumption increases with increasing distance from tree stems.

In order to fully make use of the results of Frandsen (1997) in developing a spatial model of duff consumption, one must have an understanding of how soil conditions vary in space and time. Of particular interest is duff moisture. Duff moisture is recognized as an important predictor of how duff is consumed since the limits of smoldering combustion are determined largely by moisture content (Miyanishi, 2001; Frandsen, 1987). Hille and den Ouden (2005) demonstrate the importance of moisture content as a predictor of humus consumption in Central European Scots pine (*Pinus sylvestris*) stands. Temperature dynamics affect fuel bed characteristics as higher soil temperatures drive off moisture, making the

duff more susceptible to combustion. Soil moisture also acts as a heat sink since water has a high latent heat of vaporization (Miyanishi, 2001). Thus high moisture content acts as a buffer against combustion. Heat and moisture dynamics significantly influence how duff is consumed. Therefore, a model of duff consumption should account for how heat passes through soil and drives off moisture.

The model of de Vries (1958) is a seminal work in modeling the transport of heat and moisture in porous media and serves as a prototype for countless models in soil physics, including the work of Campbell et al. (1995). The model of de Vries (1958) makes the distinction between *liquid* and *vapor* flux since both make different contributions to the transport of thermal energy in the soil. At high temperatures, water vapor transports a significant amount of thermal energy through the soil (de Vries, 1958). Cahill and Parlange (1998) develop a model for temperature and moisture dynamics in field soils that is based upon the work de Vries (1958) to show that vapor flux contributes significantly to the total moisture and energy flux in field soils. Efforts to model the more extreme temperature dynamics of fire situations include Steward et al. (1990) in which a simple one-dimensional model of heat transfer in soil is used to predict the depth at which temperatures are lethal to soil organisms. However, the model of Steward et al. (1990) is too simple in that it does not account for moisture transport. Campbell et al. (1995) simulate heat and moisture transport in soil under fire conditions and is successful in predicting soil temperature. However, the model of Campbell et al. (1995) does not perform as well when predicting soil moisture. Since the primary focus of Campbell et al. (1995) was to predict lethal heat penetration of the mineral soil, the model is considered satisfactory despite the less than satisfactory results concerning moisture dynamics. Hungerford et al. (1996) cites the model of Campbell et al. (1995) as one of the only models useful for high temperature situations. Campbell et al. (1995) note that a different version of the model based upon different mass flow as-

assumptions is a better predictor of moisture content. The details of modifications to the mass flow assumptions are not reported and were said to increase the complexity of the model. Other models created specifically for fire (high temperature) situations such as Aston and Gill (1976) can be very poor predictors of moisture. The model of Aston and Gill (1976) is too specific to the data to which the model was calibrated (Hungerford et al., 1996; Campbell et al., 1995). Hungerford et al. (1996) note that when applied to other situations, the model agreed poorly with observation and exhibited instability. Previous modeling efforts suggest that moisture dynamics are one of the more troubling aspects in modeling heat and mass transfer in soils.

The difficulties that arise in modeling moisture transport in soil stem from the complex structure of soils that vary greatly from one type of soil to another. Soils vary in the shape of granules, granule size distributions, granule composition, and the arrangement and orientation of granules. These characteristics influence how moisture moves through and is retained by the soil. Saturated soils are more prone to release moisture than dry soils, in a manner similar to that of a sponge. This trend of increasing difficulty in removing moisture from soil with decreasing moisture is measured by the *water potential* of the soil and is an important consideration when modeling moisture transport phenomena in soils (Hillel, 1998). Van Genuchten (1980) derives a closed form relationship between water potential and volumetric moisture content involving several parameters that are empirically derived. Naasz et al. (2005) fits the model of van Genuchten to wetting and drying data of peat and pine bark. The model of van Genuchten (1980) is one of several model prototypes describing water potential versus moisture content. A review of these models may be found in Hillel (1998). Campbell et al. (1995) also give a relationship between water potential and volumetric moisture content for low moisture content. Given the variety of models, it is not surprising that there is no general relationship between water potential and moisture

content that can be derived using only structural properties of soils (Hillel, 1998).

Another of the more difficult aspects in modeling heat transfer in soils and other porous media is thermal conductivity, which can be thought of as a measure of the ease with which thermal energy flows through a material. Both Cosenza et al. (2003) and Tarnawski et al. (2000) note that much of the difficulty in predicting thermal conductivity of soils stems from the scarcity of experimental data with which to validate new models which is especially true for thermal properties at higher temperatures (Tarnawski et al., 2000). The classic model of de Vries (1963) is the prototype for many “mixing” models that use a weighted sum of the thermal conductivities of the various soil components. Calculation of these weighting coefficients involves the shape and size of soil particles. Campbell et al. (1994) use a modification of de Vries (1963) in their temperature dependent model of thermal conductivity which is used in the heat and moisture transport model of Campbell et al. (1995). Other methods such as ones developed by Balland and Arp (2005) are modifications of another more empirical prototypical model developed by Johansen (1975). Volumetric fraction of air is also a good predictor of thermal conductivity (Ochsner et al., 2001). Thermal conductivity of soil is important to a successful model of heat transfer in the soil and is highly variable due to its sensitivity to water content, bulk density, porosity, chemical composition, and soil structure.

Most thermal conductivity models are not valid for temperatures that occur in wild-land fires. Frandsen (1991) notes that smoldering ground fires elevate underlying mineral soil to temperatures above 300°C with temperatures as high as 600°C. The thermal conductivity model of Balland and Arp (2005) is valid for temperature ranges between only -30°C and 30°C. Another model by Hiraiwa and Kasubuchi (2000) is valid in a temperature range from 5°C to 75°C. The thermal conductivity model developed by Cosenza et al. (2003) agrees well with simulated and collected data. A particularly appealing feature of

the model is that it is easy to use. However, the model of Cosenza et al. (2003) is perhaps inappropriate for heat transfer in duff since it does not consider low thermal conductivity in organic materials and does not account for extreme temperatures. The formulation of thermal conductivity given by Campbell et al. (1994) does take extreme temperatures into account and is better suited to modeling fire situations. The deV-1 model and deV-2 model (a detailed account of both may be found in Tarnawski et al. (2000)) are also suited to situations involving higher temperatures and have been tested against several data sets. The model takes varying mineralogy into account by partitioning the mineral contribution to thermal conductivity into several common mineral soil constituents including quartz, feldspar, and clay minerals. Since duff is composed mostly of organic material, the level of detail given to the mineral constituent of the soil by the deV-1 model is considered to be unnecessary for the present work. Therefore, the model of Campbell et al. (1994) is considered to be the most appropriate formulation of soil thermal conductivity for heat transfer in duff.

The model developed in the following pages is based upon the work of Frandsen (1997). Frandsen's empirical result is coupled with the results of Campbell et al. (1994, 1995). The model uses a slightly modified version of the model of soil thermal conductivity developed by Campbell et al. (1994). The use of these results require that the model input include organic bulk density, moisture content, and inorganic content. Since duff depth influences the efficiency with which heat is transferred into the duff (Miyaniishi, 2001), duff depth is also included as model input.

MODEL

Due to the complexity of combustion chemistry and the consequent difficulties in modeling combustion deterministically, the combustion process is modeled stochastically. However, patterns of heat and moisture transport are described well by deterministic models. Although soil structure and composition vary greatly from one soil type to another, and heat and moisture transport models in soil are sensitive to these variations, some relief is afforded to modeling heat and moisture transport in forest duff. Peat has been widely studied, and Frandsen (1987, 1991, 1998) repeatedly notes that peat has similar structural characteristics to forest duff including particle size distributions. Miyanishi (2001) also cites studies showing that peat is chemically similar to that of the fermentation horizon in duff. Therefore, it is assumed that the physical characteristics of peat including mass and thermal transport properties are similar enough to act as a surrogate for forest duff.

The overall structure of the model is a spatial lattice upon which the above processes are coupled (Figure 2). The spread of the simulated ground fire is governed by a probability. The propagating, smoldering region imparts thermal energy to the soil ahead of the front which drives off moisture. Decreasing moisture ahead of the smoldering front influences the probability of spread.

The Fuel Bed

The choice of model for the fuel bed is a two-dimensional stochastically updated cellular automaton. A particularly appealing advantage of this model choice is that stochastic processes are easily coupled with numerical schemes for simulating deterministic processes. For a broad introduction to stochastic spatial models see Durrett (1999).

Cellular automata are discrete in both time and space. More specifically, a cellular

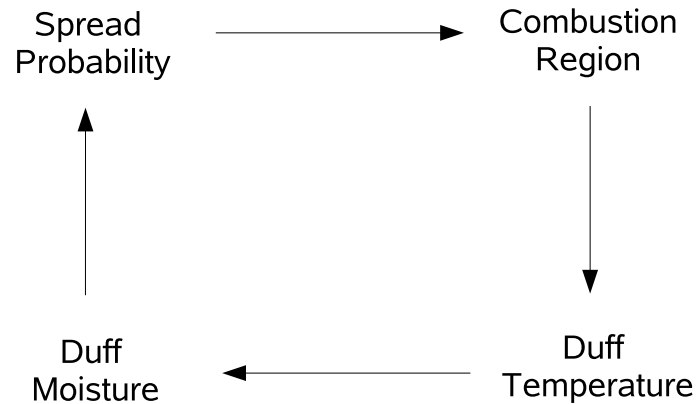


Figure 2: Overall model structure for predicting the spatial pattern of forest floor duff consumption.

automaton is a multi-dimensional lattice of cells that is updated in discrete time. With each cell is associated a *state*. The state of each cell is updated using information about itself and neighboring cells. This model updates each cell using information about itself and its *four nearest neighbors* (Figure 3). Another common configuration uses the eight nearest neighbors of a cell. The rule used to update the state of a cell may be deterministic or stochastic.

The lattice of cells represents a square grid of uniformly spaced points in \mathbb{R}^2 with cell (1,1) acting as the origin. The vertical and horizontal distance between adjacent cells is denoted by Δx so that cell (i, j) occupies the point $(x_i, y_j) = ((i - 1)\Delta x, (j - 1)\Delta x)$. The time elapsed between each time step is denoted Δt .

The state of each cell is a vector whose components are soil conditions that change in time: the stage of combustion, duff moisture, and duff temperature. Also associated with each cell are quantities that do not change in time: organic bulk density, mineral content,

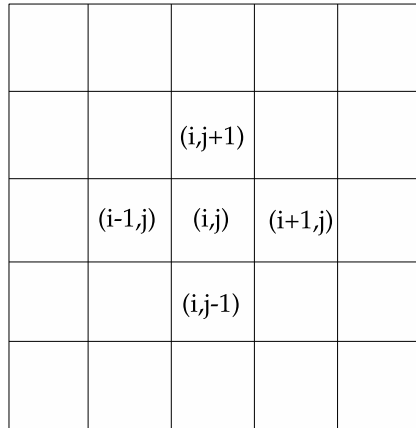


Figure 3: Cell (i, j) and its four nearest neighbors.

and duff thickness. Quantities that change in time are denoted with the subscript t .

The combustion process is modeled by three stages (or states): unburned, burning, and burned (Figure 4). Cells undergoing combustion can ignite unconsumed cells. If one or more nearest neighbors of an unconsumed cell are burning, then the cell will undergo a transition from unburned to burning with a probability determined by the conditions of the cell. The cell burns until all the fuel is consumed, at which time it transitions from the burning state to the burned state.

The duff conditions determining the ignition probability are organic bulk density, mineral content, and duff moisture. Organic bulk density, $\rho^{i,j} \left(\frac{\text{kg}}{\text{m}^3} \right)$, is the mass of an undisturbed sample of duff divided by the volume of the sample. The mineral content, $\alpha^{i,j} \left(\frac{\text{kg}}{\text{kg}} \right)$, is the mass fraction of inorganic material in the duff. Duff moisture is measured in two ways: as a volumetric ratio or gravimetric (or mass) ratio of water to dry soil. The volumetric moisture content (VMC) is denoted $\theta_t^{i,j} \left(\frac{\text{m}^3}{\text{m}^3} \right)$ and the gravimetric moisture content (GMC) is denoted $\gamma_t^{i,j} \left(\frac{\text{kg}}{\text{kg}} \right)$. The ignition probability is expressed in terms of GMC rather

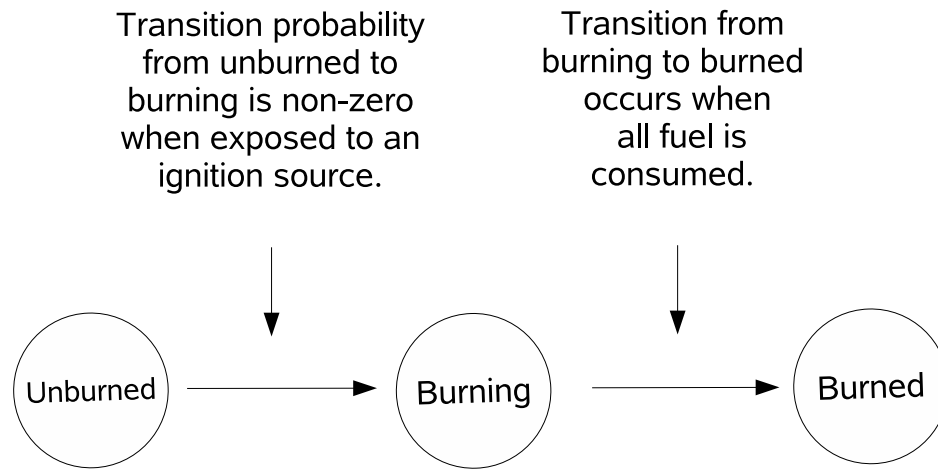


Figure 4: Three stage model of the combustion process in forest duff.

than VMC. However, VMC, rather GMC, is used almost exclusively by soil physicists in models involving moisture and heat transport. Therefore, this model uses both GMC and VMC. Note that for the convenience of the reader, a list of variables, parameters, constants, abbreviations, and their units begins on page ix in the nomenclature section.

Other duff characteristics used in the model are expressed in terms of quantities already mentioned above: dry soil bulk density $\delta^{i,j}$ $\left(\frac{\text{kg}}{\text{m}^3}\right)$ and soil porosity $\pi^{i,j}$ $\left(\frac{\text{m}^3}{\text{m}^3}\right)$. Dry bulk density is the mass of a dry soil sample divided by the volume of the sample. Soil porosity is the volumetric fraction of air in dry soil and is used to model thermal properties of the soil. The amount of organic material present per unit volume in the soil may be obtained by subtracting the amount of inorganic material per unit volume. Thus, organic bulk density is the dry soil bulk density δ minus the inorganic bulk density $\alpha\delta$, that is, $\rho = \delta - \alpha\delta$, thus $\delta = \frac{\rho}{1-\alpha}$. Porosity may be expressed in terms of dry soil bulk density and organic bulk density as $\pi = 1 - \frac{\alpha\delta}{d_m} - \frac{\rho}{d_o}$ where d_m and d_o are the respective densities $\left(\frac{\text{kg}}{\text{m}^3}\right)$ of inorganic

and organic matter in the duff.

Duff moisture is necessary for determining the ignition probability in unconsumed cells. Consequently, the model monitors the amount of thermal energy imparted to the duff by the smoldering front which then drives off moisture. Therefore, the temperature $T_t^{i,j}$ (K) of the duff for each time step is calculated. Duff thickness influences the efficiency at which the smoldering front imparts thermal energy to unconsumed duff (Miyanishi and Johnson, 2002). Thus also associated with each cell is a thickness $\tau^{i,j}$ (m).

Initialization

Organic bulk density, mineral content, moisture content and thickness of the duff layer may be stochastically initialized to simulate a typical fuel bed found in the field. Determining how these quantities vary in soil, however, is a difficult problem. Certainly these quantities are not independent of one another. For example, smaller bulk density allows for greater moisture content. Also, there is the issue that one would expect to see less variation in soil characteristics on a smaller (within-site) scale. For example, one would expect that neighboring 1 cm by 1 cm squares to a very wet 1 cm by 1 cm square of soil would also be comparably wet. Thus cells cannot simply be initialized independently of one another. Initializing duff layer characteristics presents its own difficulties and could occupy a volume of its own. One of the benefits of a lattice model is that better initialization strategies are easily incorporated into the model if such a scheme becomes necessary.

Fortunately, the initialization problem presents little difficulty in comparing the model to laboratory studies. Uniform initial conditions may be used to test the model against empirical studies since these studies often use peat samples of uniform composition. For this work, uniform conditions are assumed so that for all (i, j) , $\rho^{i,j} = \mu_\rho$, $\gamma_0^{i,j} = \mu_\gamma$,

$\alpha^{i,j} = \mu_\alpha$, and $\tau^{i,j} = \mu_\tau$ where μ_ρ , μ_γ , μ_α , and μ_α are the field means of the subscripted quantity.

Temperature and Moisture Dynamics

A continuous model of heat and moisture dynamics is developed. The resulting system of partial differential equations is then discretized. Temperature and moisture are updated using this discretized system. As is common, the soil (duff) is treated as a mixture of various components, namely mineral solids, organic solids, air, and water. The present model uses a modified version of the model developed by Campbell et al. (1994, 1995) of heat and moisture transport in soil. The modifications make use of deV-1 thermal conductivity model detailed by Tarnawski et al. (2000).

Campbell et al. (1995) developed a one-dimensional model coupling temperature and moisture in a soil column assuming negligible liquid flux

$$C \frac{\partial T}{\partial t} - H d_w \frac{\partial \theta}{\partial t} = \frac{\partial}{\partial z} \left(K \frac{\partial T}{\partial z} \right) \quad (1)$$

$$d_w \frac{\partial \theta}{\partial t} = - \frac{\partial}{\partial z} \left(\frac{V}{1 - \frac{p}{P_a}} \frac{\partial p}{\partial z} \right) \quad (2)$$

where T is temperature measured with the Kelvin (K) scale, θ is the volumetric moisture content of the soil $\left(\frac{\text{m}^3}{\text{m}^3} \right)$, C is the volumetric heat capacity of the soil $\left(\frac{\text{J}}{\text{m}^3 \text{K}} \right)$, K is the thermal conductivity of the soil $\left(\frac{\text{J}}{\text{m hr K}} \right)$, H is the latent heat of vaporization of water $\left(\frac{\text{J}}{\text{kg}} \right)$, d_w is the density of liquid water $\left(\frac{\text{kg}}{\text{m}^3} \right)$, p is the partial pressure of water vapor in the soil (Pa), P_a is ambient pressure, and V is the vapor conductivity of the soil $\left(\frac{\text{kg}}{\text{m Pa hr}} \right)$. Note that this model uses different time units than Campbell et al. (1995) since smoldering combustion is a very slow process (linear smolder velocities are on the order of $10^{-2} \frac{\text{m}}{\text{hr}}$).

The term $-Hd_w \frac{\partial \theta}{\partial t}$ accounts for transport of thermal energy due to water vapor moving through the soil. The term $\frac{1}{1-\frac{p(T)}{P_a}}$ is called the *Stefan correction* which is a mass flow correction that accounts for the flow of water vapor induced by the movement of air in the soil (Ghildyal and Tripathi, 1987). Also, note that θ is the sum of the volumetric fractions of liquid water and precipitable water vapor (the volumetric fraction of condensed water vapor).

An empirically derived equation used by Campbell et al. (1995) expresses H in terms of temperature and water potential in the units of $\frac{\text{J}}{\text{mol}}$ as $H = 45144 - 48(T - 273.15) - 0.018\psi$ where ψ is the water potential $\left(\frac{\text{J}}{\text{kg}}\right)$ of the soil.

Soil water potential is essential to describing how moisture moves through soil and quantifies the trend of increasing difficulty in removing moisture from soil with decreasing moisture. Water moves from regions of high water potential to regions of lower potential (Hillel, 1998). Since water in saturated regions of soil tends to flow to regions of soil that are less saturated, dry soil has a more negative water potential than that of a wet soil. Saturated soils, the point where water is no longer drawn into the soil, have a water potential of zero so that the water potential in non-saturated (dry and moist) soils is a negative quantity. Oven dried soils have water potentials on the order of $\psi = -10^6 \frac{\text{J}}{\text{kg}}$ (Campbell et al., 1995).

The vapor conductivity V of the soil is expressed by Campbell et al. (1995) as $V = \frac{\xi\eta(\pi-\theta)M_w D_v}{RT}$ where M_w is the molecular weight of water $\left(\frac{\text{kg}}{\text{mol}}\right)$ and R is the universal gas constant $\left(\frac{\text{mol}}{\text{K}}\right)$. ξ is a *tortuosity* correction. The tortuosity of a soil is the ratio of the straight line distance from one location to another to how far a fluid actually travels (Hillel, 1998). η is a vapor flow enhancement factor, and $\pi - \theta$ is the air filled pore space. D_v is the diffusivity of water vapor in air $\left(\frac{\text{m}^2}{\text{hr}}\right)$ and is related to temperature and the ambient pressure by $D_v = D_{v0}\left(\frac{P_0}{P_a}\right)\left(\frac{T}{T_0}\right)^{7/4}$ where D_{v0} is the diffusivity and P_0 is the ambient pressure

at standard temperature and pressure.

Campbell et al. (1995) note that the relationship between p and θ is not unique. To account for this, the partial pressure of water is expressed as the product of relative humidity h and the saturation vapor pressure P , $p = hP$. Campbell et al. (1995) note that the saturation vapor pressure of water is a function of temperature alone and state an empirically derived formula for P in terms of T given by

$$P(T) = 101325e^{13.3016S(T)-2.042S(T)^2+0.26S(T)^3+2.69S(T)^4}$$

where $S(T) = 1 - \frac{373.15}{T}$. The humidity is expressed in terms of the water potential and temperature of the soil as $h = e^{\frac{M_w\psi}{RT}}$.

Equations (1) and (2) are modified to model a two-dimensional fuel bed of duff instead of a one-dimensional soil column. Temperature and moisture gradients drive both vertical and horizontal transport of heat and moisture in porous media (de Vries, 1958) (vertical transport requires also the consideration of gravitation). The derivation of Equations (1) and (2) by Campbell et al. (1995) is essentially the same as the derivation of the multi-dimensional model of heat and moisture transport by de Vries (1958). Thus the one-dimensional vertical gradient $\frac{\partial}{\partial z}$ is replaced by the two-dimensional gradient operator $\nabla = \left(\frac{\partial}{\partial x}, \frac{\partial}{\partial y}\right)$. Taking convective cooling at the surface of the duff into account, the continuous model for heat and moisture transport in unconsumed duff is

$$C \frac{\partial T}{\partial t} - \zeta H d_w \frac{\partial \theta}{\partial t} = \nabla \cdot (K \nabla T) - \kappa_c C (T - T_a) \quad (3)$$

$$d_w \frac{\partial \theta}{\partial t} = -\nabla \cdot \left(\frac{V}{1 - \frac{p}{P_a}} \nabla (p(T)) \right) \quad (4)$$

for $(x, y) \in \mathcal{U} \subseteq [0, L] \times [0, L] = \mathcal{F}$ where \mathcal{U} is the unconsumed region of duff, and \mathcal{F}

is the entire L by L fuel-bed. κ_c is a convective cooling constant, and T_a is the ambient temperature. Notice that in the absence of space and moisture considerations, Equation (3) reduces to Newton's Law of Cooling with κ_c as the cooling constant. The burned region $\mathcal{F} \setminus \mathcal{U}$ is updated stochastically. A continuous rule is not developed for how this region changes through time. The rule governing how the consumed region $\mathcal{F} \setminus \mathcal{U}$ changes through time is more naturally accomplished in a discrete setting. Under the conditions of this model, the heat and moisture transport model of Campbell et al. (1995) over predicts the amount of thermal energy carried off by water vapor, therefore, parameter ζ is introduced to scale back energy flux due to vapor flux.

Since moisture content is used to update ignition probability, it becomes unnecessary to update after a cell is undergoing consumption. In smoldering and consumed regions, $\mathcal{F} \setminus \mathcal{U}$, θ is set to a specified minimum value θ_{min} . In the smoldering regions the temperature is set to a constant value T_c , representing the temperature at which duff undergoes combustion. The model uses a combustion temperature of 400°C (Miyanishi, 2001). When combustion ceases, the temperature decays to the ambient temperature according to Newton's Law of Cooling. Temperature and VMC at the boundary of \mathcal{F} are assumed to be the ambient temperature and initial VMC. The above establishes boundary conditions for the temperature and moisture dynamics at the ever-changing boundary of unconsumed soil.

In an effort to simplify the numerical scheme, it is advantageous to compute water potential directly from VMC. Each soil exhibits a one-to-one relationship between VMC and water potential and this is termed as the soil's *water retention curve* (Hillel, 1998). One such relationship proposed by van Genuchten (1980) is appropriate in very moist soils. The numerical scheme used by Campbell et al. (1995) uses a linear relationship between θ and $\ln(\psi)$ for low soil moisture to estimate VMC from water potential. Since the VMC of duff that could potentially sustain smoldering combustion is relatively low (less than 30%), the

above relationships and those reviewed by Hillel (1998) may be used to estimate water potential from VMC. However, there is no apparent change in model behavior when the water potential is allowed to vary between $\psi \approx -10^6$ for dry duff and $\psi \approx -3 \times 10^5$ for moist duff, according to the empirical relation $\psi = a\theta^{-b}$ cited by Hillel (1998), where a and b are fitting parameters. Therefore, to improve the stability of the numerical scheme, the water potential is assumed to be a constant value of $\psi = -10^6 \frac{\text{J}}{\text{kg}}$.

It is noted that due to extreme temperatures of the combustion process, the above model often predicts partial pressures of water vapor in excess of the ambient pressure yielding negative values of the Steffan correction and hence unreasonable values for the vapor conductivity. The Steffan correction is positive when $0 \leq p < P_a$. Therefore, the partial pressure of water vapor is assumed to not exceed some value close to the ambient pressure. A value of $0.9P_a$ works well and yields reasonable results. Thus, $p = \min\{hP, 0.9P_a\}$. The above restriction also has a stabilizing effect on the numerical scheme by limiting the Steffan correction to values less than 10. Campbell et al. (1995) impose a similar restriction on the Steffan correction (to values less than 3.3) with reasonable results and numerical stability.

Equations (3) and (4) and the boundary conditions described above serve as the continuous thermal and moisture transport model in unconsumed duff. The model equations are discretized to develop update rules for duff temperature and moisture on the cellular lattice described above.

Update Rules

Combustion State

The transition probabilities between the three states unburned, burning and burned are derived to obtain an update rule for the combustion state. This update rule is summarized by Figure 4. The states unburned, burning and burned are respectively denoted as 0, 1, and 2. Since combustion is a forward process, transitions from burned to burning, burning to unburned, and burned to unburned are impossible. Denoting the burn state of cell (i, j) at time-step t as $\beta_t^{i,j}$, these statements are expressed as $\mathcal{P}([\beta_{t+1}^{i,j} = 1] \mid [\beta_t^{i,j} = 2]) = 0$, $\mathcal{P}([\beta_{t+1}^{i,j} = 0] \mid [\beta_t^{i,j} = 1]) = 0$, and $\mathcal{P}([\beta_{t+1}^{i,j} = 0] \mid [\beta_t^{i,j} = 2]) = 0$. Also, a cell must undergo combustion before it can be completely consumed, so a transition from unburned to burned is also impossible, so $\mathcal{P}([\beta_{t+1}^{i,j} = 2] \mid [\beta_t^{i,j} = 0]) = 0$.

To derive the transition probability from 0 to 1, it must first be determined whether or not a particular cell is exposed to an ignition source. Cell (i, j) at time t is considered to be exposed to an ignition source if at least one of its four nearest neighbors is burning. Thus, an indicator variable $E_t^{i,j}$ is defined to be 1 when $\beta_t^{i-1,j} = 1$, $\beta_t^{i+1,j} = 1$, $\beta_t^{i,j-1} = 1$, or $\beta_t^{i,j+1} = 1$, and is 0 otherwise. If a cell is not exposed to an ignition source ($E_t^{i,j} = 0$), then a transition from state unburned to burning is impossible. This is expressed as $\mathcal{P}([\beta_{t+1}^{i,j} = 1] \mid [\beta_t^{i,j} = 0] \cap [E_t^{i,j} = 0]) = 0$. The probability statement developed by Frandsen (1997) is used to develop an expression for $\mathcal{P}([\beta_{t+1}^{i,j} = 1] \mid [\beta_t^{i,j} = 0] \cap [E_t^{i,j} = 1])$.

Frandsen (1997) models the probability of complete consumption of a sample of duff after sufficient exposure to an ignition source in terms of the sample's organic bulk density, ρ , gravimetric moisture content, γ , and percentage inorganic content, α . Denoting the event of complete consumption by smoldering combustion by C , the above probability is given

by

$$\mathcal{P}(C) = \frac{1}{1 + e^{-(B_0 + B_1\gamma + B_2\alpha + B_3\rho)}}$$

where the parameters B_0 , B_1 , B_2 , and B_3 are determined by binary logistic regression for a particular type of duff (Frandsen, 1997). Since each cell represents a small patch of duff, it is reasonable to assume that the probability of a cell undergoing ignition in the next time-step when exposed to a burning cell is related to the above probability. The distance between cells (Δx) and the time elapsed between time-steps (Δt) also influences the probability of spread. The model assumes that the ignition probability between adjacent cells for a given Δx and Δt is proportional to the probability given by Frandsen (1997), that is

$$\mathcal{P}([\beta_{t+1}^{i,j} = 1] \mid [\beta_t^{i,j} = 0] \cap [E_t^{i,j} = 1]) = \frac{\chi}{1 + e^{-(B_0 + B_1\gamma_t^{i,j} + B_2\alpha_t^{i,j} + B_3\rho_t^{i,j})}}$$

where χ is a scaling parameter determined by Δx and Δt . χ determines an average simulated smolder velocity Λ on the lattice. Therefore, for a desired smolder velocity, Λ is also used to determine χ . An expression for χ in terms of Δx , Δt , and Λ is developed later in this section.

If a cell is burning, it will continue to burn provided there is fuel to be consumed and will pass to the burned state when no fuel remains. Instead of modeling directly the consumption of fuel, a model for the time a cell undergoes combustion is constructed. The consumption time remaining for cell (i, j) at time-step t is denoted $\Theta_t^{i,j}$. How to determine the consumption time will be discussed later in this section. Therefore, $\mathcal{P}([\beta_{t+1}^{i,j} = 1] \mid [\beta_t^{i,j} = 1] \cap [\Theta_t^{i,j} > 0]) = 1$ and $\mathcal{P}([\beta_{t+1}^{i,j} = 2] \mid [\beta_t^{i,j} = 1] \cap [\Theta_t^{i,j} \leq 0]) = 1$. All other transition probabilities may be deduced from the ones derived above.

Under optimal smoldering conditions the probability statement of Frandsen (1997) be-

tween adjacent cells may be considered to be 1. Therefore, the scaling parameter χ induces an *uninhibited* simulated smolder velocity on the lattice. Since simulated smolder velocities should reflect observed smolder velocities, a rule for determining the value of χ that gives a desired uninhibited simulated smolder in velocity Λ is developed. A one-dimensional lattice is considered first. The results are then adapted to a two-dimensional lattice.

Consider a one-dimensional lattice of equally spaced cells a distance of Δx units length apart that updates every Δt time units. Suppose that cell i undergoes ignition and that there is a fixed probability χ of propagation from cell i to the adjacent cell $i + 1$ for each subsequent time step. Considering only rightward propagation, suppose m cells undergo ignition in n time steps. Then the “front” has traveled $m\Delta x$ units length over an elapsed time of $n\Delta t$ time units. Then the “average smolder velocity” Λ is $\frac{m\Delta x}{n\Delta t}$. But $\frac{m}{n}$ is an approximation of χ by virtue of how χ is defined. Thus the average smolder velocity Λ on the one-dimensional lattice is taken to be $\Lambda = \chi \frac{\Delta x}{\Delta t}$. The desired probability is then $\chi = \Lambda \frac{\Delta t}{\Delta x}$. Thus, on a one-dimensional lattice, the scaling parameter, χ , that yields an *uninhibited* average smolder velocity of Λ is

$$\chi = \Lambda \frac{\Delta t}{\Delta x}.$$

Obtaining an analytic result concerning the scaling parameter χ that gives a desired average smolder velocity on a two-dimensional lattice is a difficult problem. Due to the difficulty of the problem, this work constructs a statistical model that predicts the scaling parameter that gives a desired uninhibited linear smolder velocity on a two-dimensional lattice. With the results of one-dimensional lattice in mind, it is not surprising that $\chi \frac{\Delta x}{\Delta t}$ is useful in predicting the linear velocity of a simulated smoldering front on a two-dimensional lattice.

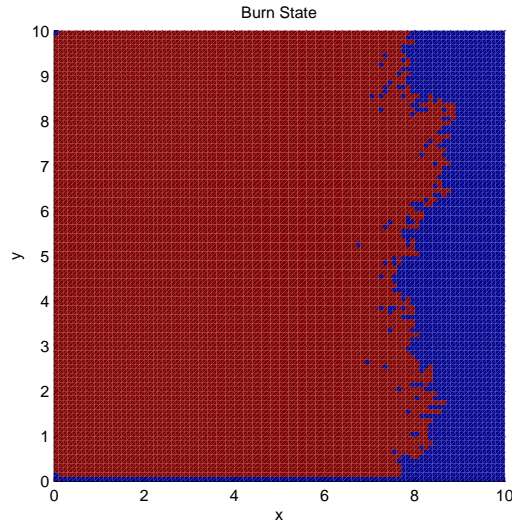


Figure 5: The uninhibited smoldering front (with the initial burn edge on the left) when 80% of cells have become active.

On a two-dimensional lattice with cells spaced Δx meters apart and updated every Δt hours, a spread probability χ induces an “average” smolder velocity Λ . For varying values of Δx , Δt , and χ , an uninhibited smolder velocity Λ was observed. The smolder velocity simulations consisted of allowing a smoldering front in two dimensions to proceed uninhibited from one side (in this case the left edge) of an L by L square (Figure 5). For all simulations, L was taken to be 10 meters. Note the choice of L is arbitrary since the smolder velocity will depend upon the distance between cells Δx and the time elapsed between each time step Δt . The simulation ends when 80% of the cells have changed from inactive to active (i.e., burning). The average distance from the initial burn edge was taken to be the burn area (number of active cells $\times (\Delta x)^2$) divided by L . The slope of the regression line through these points (Figure 6) is taken to be the average smolder velocity. The stochasticity of the smolder velocity is apparent from plots of average distance versus time (Figure 6). Multiple simulations were carried out for each combination of the values

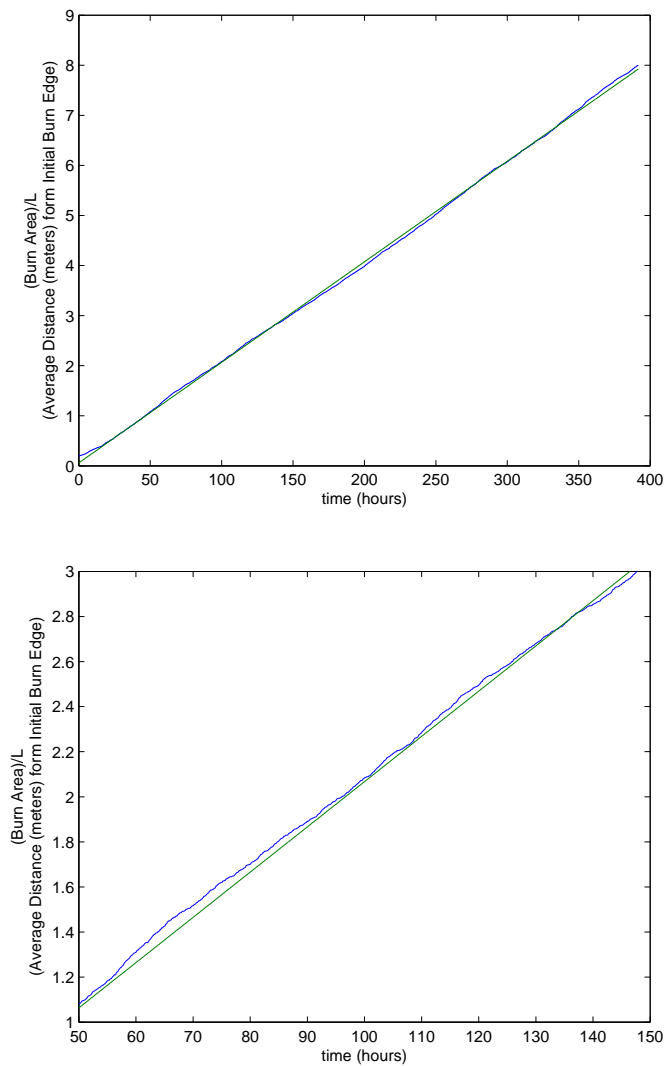


Figure 6: The average distance from the initial burn edge (left) versus time (blue). The slope of the regression line (green) is taken to be the average smolder velocity. The lower graph (50-150 hours) is a magnification of the upper graph (0-400 hours).

$\Delta x = 0.05, 0.06666, 0.1, 0.2$; $\Delta t = 0.1, 0.3, 0.5, 0.7, 0.9$; $\chi = 0.01, 0.02, 0.03, 0.04, 0.05$. The sample mean of the observed smolder velocities for n trials was taken to be the average smolder velocity associated with the particular values of Δx , Δt , and χ . For larger sample standard deviations in the average smolder velocity, more trials were run.

Several regression models were considered to predict the average smolder velocity in terms of Δx , Δt , and χ . Since $\chi \frac{\Delta x}{\Delta t}$ is the average smolder velocity in one dimension, it is reasonable that this quantity would also be a good predictor of the average smolder velocity in two dimensions. The model $\Lambda = S_0 + \chi \frac{\Delta x}{\Delta t}$ yields a good fit with an adjusted R^2 value of 0.99. However, including Δx and Δt as parameters accounts for even more of the variation in the average smolder velocity. The model

$$\Lambda = S_0 + S_1 \chi \frac{\Delta x}{\Delta t} + S_2 \Delta x + S_3 \Delta t$$

where $S_0 = 0.0021$, $S_1 = 1.90$, $S_2 = -0.00476$, and $S_3 = -0.00185$, yields an *excellent* fit to the data with an adjusted R^2 of *at least* 0.99 (very close to 1). The scaling parameter χ may then be predicted by solving for χ in the above regression equation

$$\chi = \frac{\Delta t}{S_1 \Delta x} (\Lambda - S_0 - S_2 \Delta x - S_3 \Delta t).$$

The average smolder velocity induced by χ is taken to be an uninhibited (or dry) smolder velocity since $\mathcal{P}([\beta_{t+1}^{i,j} = 1] | [\beta_t^{i,j} = 0] \cap [E_t^{i,j} = 1]) = \frac{\chi}{1 + e^{-(B_0 + B_1 \gamma_t^{i,j} + B_2 \alpha_t^{i,j} + B_3 \rho_t^{i,j})}} \approx \chi$ for dry soil conditions (for dry soil conditions $\frac{1}{1 + e^{-(B_0 + B_1 \gamma_t^{i,j} + B_2 \alpha_t^{i,j} + B_3 \rho_t^{i,j})}} \approx 1$).

Linear smolder velocities of ground fires are typically on the order of $0.03 \frac{\text{m}}{\text{hr}}$ (Frandsen, 1991). The uninhibited smolder velocity Λ is therefore taken to be equal to $0.05 \frac{\text{m}}{\text{hr}}$ for all simulations since this yields an uninhibited simulated smolder velocity of about $0.03 \frac{\text{m}}{\text{hr}}$

under dry field conditions.

Once a cell becomes active, it must be determined how long that cell stays active, that is, how long it burns. Since life-span, times between certain events, and failure times are often modeled well by an exponential distribution (Ross, 2005), it is reasonable that the duration of smoldering in a given cell be modeled by a random variable $\Theta \in [0, \infty)$ with probability density function

$$f_{\Theta}(t) = \frac{1}{\lambda} e^{-\frac{t}{\lambda}}$$

where the parameter λ is determined by the characteristics of the lattice and the duff. The mean smoldering time of Θ is λ and is assumed to be proportional to the amount of time it takes for a smoldering front to travel the distance Δx on the lattice which is on average $\frac{\Delta x}{\Lambda}$. This average smoldering time is then scaled by a dimensionless proportionality constant ϑ . Therefore, $\lambda = \vartheta \frac{\Delta x}{\Lambda}$. Thus, the burn time is initialized to

$$\Theta_0^{i,j} = -\vartheta \frac{\Delta x}{\Lambda} \ln(U)$$

where $U \in [0, 1]$ is a uniform random variable, and is updated according to the rule

$$\Theta_{t+1}^{i,j} = \begin{cases} \Theta_t^{i,j} - \Delta t, & \text{if } \beta_t^{i,j} = 1 \\ \Theta_t^{i,j}, & \text{if } \beta_t^{i,j} \neq 1. \end{cases}$$

Once the the duration time has expired (when $\Theta_t^{i,j} \leq 0$) the cell is considered to be burned.

The above considerations are summarized by the update rule for the combustion state:

$$\beta_{t+1}^{i,j} = \begin{cases} 0 & \text{if } \beta_t^{i,j} = 0 \text{ and } E_t^{i,j} = 0 \\ 0 & \text{if } \beta_t^{i,j} = 0, E_t^{i,j} = 1, \text{ and } U > \frac{\chi}{1+e^{-(B_0+B_1\gamma_t^{i,j}+B_2\alpha^{i,j}+B_3\rho^{i,j})}} \\ 1 & \text{if } \beta_t^{i,j} = 0, E_t^{i,j} = 1, \text{ and } U < \frac{\chi}{1+e^{-(B_0+B_1\gamma_t^{i,j}+B_2\alpha^{i,j}+B_3\rho^{i,j})}} \\ 1 & \text{if } \beta_t^{i,j} = 1 \text{ and } \Theta_t^{i,j} > 0 \\ 2 & \text{if } \beta_t^{i,j} = 1 \text{ and } \Theta_t^{i,j} \leq 0 \\ 2 & \text{if } \beta_t^{i,j} = 2 \end{cases} \quad (5)$$

where $U \in [0, 1]$ is a uniform random variable.

Volumetric Moisture Content

Equation (4) is discretized first to develop an update rule for VMC, since updating temperature will require an updated VMC. The combustion state must also be updated before temperature since thermal energy is supplied to the soil at the boundary of smoldering regions and since the combustion state determines where those smoldering regions occur. The corrected vapor conductivity $\frac{V}{1-\frac{p}{P_a}}$ is not a constant, but depends upon x and y . Thus the right hand side of Equation (4) must be expanded into its component derivatives. Letting

$$v = \frac{V}{1-\frac{p}{P_a}},$$

$$\nabla \cdot (v\nabla p) = \nabla v \cdot \nabla p + v\nabla^2 p = \frac{\partial v}{\partial x} \frac{\partial p}{\partial x} + \frac{\partial v}{\partial y} \frac{\partial p}{\partial y} + v\left(\frac{\partial^2 p}{\partial x^2} + \frac{\partial^2 p}{\partial y^2}\right).$$

Equation (4) then becomes

$$d_w \frac{\partial \theta}{\partial t} = - \frac{\partial v}{\partial x} \frac{\partial p}{\partial x} - \frac{\partial v}{\partial y} \frac{\partial p}{\partial y} - v \left(\frac{\partial^2 p}{\partial x^2} + \frac{\partial^2 p}{\partial y^2} \right).$$

Using a forward difference in time and a centered difference in space, the discretized form is then

$$\begin{aligned} d_w \frac{\theta_{t+1}^{i,j} - \theta_t^{i,j}}{\Delta t} = & - \left(\frac{v_t^{i+1,j} - v_t^{i-1,j}}{2\Delta x} \right) \left(\frac{p_t^{i+1,j} - p_t^{i-1,j}}{2\Delta x} \right) \\ & - \left(\frac{v_t^{i,j+1} - v_t^{i,j-1}}{2\Delta y} \right) \left(\frac{p_t^{i,j+1} - p_t^{i,j-1}}{2\Delta y} \right) \\ & - v_t^{i,j} \left(\frac{p_t^{i+1,j} - 2p_t^{i,j} + p_t^{i-1,j}}{(\Delta x)^2} + \frac{p_t^{i,j+1} - 2p_t^{i,j} + p_t^{i,j-1}}{(\Delta y)^2} \right). \end{aligned}$$

Adapting the above to the cellular lattice, Δx is taken to be $\frac{L}{n}$. Since it is assumed that the horizontal and vertical spacing on the cellular lattice is equal, it is true that $\Delta y = \Delta x$.

Rearranging, the above becomes

$$\begin{aligned} \theta_{t+1}^{i,j} = & \theta_t^{i,j} - \frac{\Delta t}{4d_w(\Delta x)^2} [(v_t^{i+1,j} - v_t^{i-1,j})(p_t^{i+1,j} - p_t^{i-1,j}) + (v_t^{i,j+1} - v_t^{i,j-1})(p_t^{i,j+1} - p_t^{i,j-1})] \\ & - \frac{\Delta t v_t^{i,j}}{d_w(\Delta x)^2} [p_t^{i+1,j} + p_t^{i-1,j} + p_t^{i,j+1} + p_t^{i,j-1} - 4p_t^{i,j}] \\ := & u_\theta(S_t^{i,j}) \end{aligned}$$

where $S_t^{i,j}$ is vector consisting of each duff characteristic at cell (i, j) and its four nearest neighbors at time-step t . The model of Campbell et al. (1995) sometimes predicts negative VMCs. To avoid negative moisture values, a value $\theta_{min} > 0$ is set to be the value of lowest moisture content. The update rule in the unconsumed regions of duff (cells for which

$\beta_t^{i,j} = 0$) is then

$$\theta_{t+1}^{i,j} = \max\{u_\theta(S_t^{i,j}), \theta_{min}\}.$$

As specified earlier, θ is taken to be θ_{min} in cells that are burned or burning ($\beta_t^{i,j} \neq 0$). The update rule for VMC is then

$$\theta_{t+1}^{i,j} = \begin{cases} \max\{u_\theta(S_t^{i,j}), \theta_{min}\} & \text{if } \beta_t^{i,j} = 0 \\ \theta_{min} & \text{if } \beta_t^{i,j} \neq 0. \end{cases} \quad (6)$$

Gravimetric Moisture Content

Soil physicists most often use VMC rather than GMC in models involving heat and moisture transport. This model must use both since the probability result of Frandsen (1997) uses GMC and the modified model of Campbell et al. (1995) uses VMC. Hence, the updated VMC must be converted to GMC in order to use the result of Frandsen (1997).

Since

$$\begin{aligned} \text{VMC} &= \frac{\text{volume of water}}{\text{volume of soil}} \\ &= \frac{\text{volume of water}}{\text{mass of water}} \times \frac{\text{mass of soil solids}}{\text{volume of soil}} \times \frac{\text{mass of water}}{\text{mass of soil solids}} \\ &= \frac{1}{\text{density of water}} \times \text{bulk density of soil} \times \text{GMC}, \end{aligned}$$

VMC is expressed in terms of GMC by

$$\theta = \frac{\delta\gamma}{d_w}$$

where d_w is the density of water. From the above the update rule for GMC is

$$\gamma_{t+1}^{i,j} = \frac{d_w \theta_{t+1}^{i,j}}{\delta^{i,j}}. \quad (7)$$

Temperature

To develop an update rule for temperature, Equation (3) is discretized. First, however, the volumetric heat capacity and thermal conductivity of the duff are needed.

Volumetric heat capacity is not difficult to model as noted by Tarnawski et al. (2000). A common and effective method is treating the volumetric heat capacity as a weighted sum of the products of the volumetric fraction ϕ and volumetric heat capacity C of each soil constituent (de Vries, 1963; Ochsner et al., 2001; Balland and Arp, 2005). Notice that for water ϕ_w is merely the VMC of the soil θ . The soil is a mixture of water, air, and mineral and organic solids, thus the volumetric heat capacity of the soil is expressed as the weighted sum $C = \theta C_w + \phi_a C_a + \phi_m C_m + \phi_o C_o$. The above may be rewritten as $C = \theta d_w c_w + \phi_a d_a c_a + \phi_m d_m c_m + \phi_o d_o c_o$ where c_i and d_i are respectively the specific heat capacity $\left(\frac{\text{J}}{\text{kg K}}\right)$ and particle density of the each soil constituent. Since the mass of air is negligible in comparison to the other components of the soil, $d_a \approx 0$. Then

$$C = \theta d_w c_w + \phi_m d_m c_m + \phi_o d_o c_o$$

is the expression for volumetric heat capacity of the soil.

It is advantageous to express each volumetric fraction in terms of known duff characteristics. In general, volumetric fractions can be expressed as

$$\phi = \frac{\text{bulk density}}{\text{particle density}}$$

so that $\phi_o = \frac{\rho}{d_o}$ and $\phi_m = \frac{\alpha\delta}{d_m}$. ϕ_a may also be expressed in terms of basic soil properties. Since $\phi_w + \phi_a + \phi_m + \phi_o = 1$, it is seen that $\phi_a = 1 - \phi_w - \phi_m - \phi_o = 1 - \theta - \frac{\alpha\delta}{d_m} - \frac{\rho}{d_o}$. Note that in dry soil $\phi_w = 0$ so that the volumetric fraction of air in dry soil, that is, the soil porosity, is given by $\pi = \phi_a = 1 - \phi_w - \phi_m - \phi_o = 1 - \frac{\alpha\delta}{d_m} - \frac{\rho}{d_o}$.

As stated earlier, thermal conductivity presents significantly greater difficulty than that of volumetric heat capacity. Since a model of thermal conductivity suited to higher temperatures is desired, the methods of Campbell et al. (1994) with only slight modifications using the deV-1 model outlined in Tarnawski et al. (2000) will be employed. Note that both are adaptations of the model by de Vries (1963) treating thermal conductivity as a weighted sum involving each soil constituent. Considering the duff to be a mixture of air, moisture, mineral solids, and organic solids, this weighted sum for thermal conductivity is:

$$K = \frac{k_w\theta\lambda_w + k_a\phi_a\lambda_a + k_m\phi_m\lambda_m + k_o\phi_o\lambda_o}{k_w\theta + k_a\phi_a + k_m\phi_m + k_o\phi_o}$$

where $\lambda_w, \lambda_a, \lambda_m, \lambda_o$ are the respective thermal conductivities of water, air, minerals, and organic matter. The weighting factors k_w, k_a, k_m, k_o are determined by soil characteristics of granule shape and soil porosity. Distinguishing between organic and mineral content in soil (duff) solids is one of the modifications made here to the model by Campbell et al. (1994). The deV-1 model considers various minerals as soil constituents including feldspar, mica, quartz, and several others. However, the present model uses a single thermal conductivity for the mineral constituent of the soil. Thus, for the purposes of this model the mineral component of the duff is uniform.

To use the deV-1 and de Vries (1963) model, one must distinguish if air or water is the continuous medium of heat transfer in the soil. This dichotomous treatment of soil water saturation is cited by Tarnawski et al. (2000) as an area where the deV-1 model could use

improvement as it is one of the more cumbersome aspects of the model. By using the methods of Campbell et al. (1994) the present model circumvents this difficulty and introduces a fluid thermal conductivity λ_f which is given by $\lambda_f = \lambda_a + f_w(\lambda_w - \lambda_a)$ where f_w is an empirical weighting function. f_w is given by $f_w = \frac{1}{1+(\frac{\theta}{\theta_0})^{-q}}$ where θ_0 is an empirically determined constant particular to the soil data. Campbell et al. (1994) give values of θ_0 for several types of soil. The quantity q is temperature dependent and is given by $q = q_0(\frac{T}{303})^2$ where q_0 is also an empirically determined constant particular to the soil and is also reported for each soil type. The advantage to a fluid thermal conductivity is that instead of having just air or water as the continuous medium, there is a continuous scale of saturation from 0 to 1 for a more seamless model. For λ_w , and λ_o formulae given by the deV-1 model are used $\lambda_w = 3600 (0.569 + 1.884 \times 10^{-3}(T - 273.15) - 0.0772 \times 10^{-5}(T - 273.15)^2) \frac{\text{J}}{\text{m hr K}}$, $\lambda_o = 900 \frac{\text{J}}{\text{m hr K}}$.

Campbell et al. (1994) assume that λ_m is a constant. The same will be done here taking $\lambda_m \approx 7200 \frac{\text{J}}{\text{m hr K}}$ for the mineral content of the duff.

Campbell et al. (1994) give the apparent thermal conductivity of air in the soil (duff) as $\lambda_a = \frac{Hh f_w D_a D_v}{P_a - hP} \frac{dP}{dT}$ where D_a is the molar density of air ($\frac{\text{mol}}{\text{m}^3}$). D_a may be expressed in terms of temperature and pressure by $D_a = D_{a0} \frac{P_a T_0}{P_0 T}$ where D_{a0} is the molar density of air at standard temperature and pressure. Because vapor pressure, P , is explicitly given in terms of temperature, T , $\frac{dP}{dT}$ is easy to calculate.

The weighting factors k_w , k_a , k_o , are given by Campbell et al. (1994)

$$k_i = \frac{1}{3} \left[\frac{2}{1 + (\frac{\lambda_i}{\lambda_f} - 1)g_a} + \frac{1}{1 + (\frac{\lambda_i}{\lambda_f} - 1)(1 - 2g_a)} \right]$$

where $i \in \{w, a, o\}$. g_a is known as a *shape factor* which takes into account the the shape of the granules of each soil constituent. Campbell et al. (1994) treats g_a as a parameter to

be determined empirically and lists its estimated value for each type of soil. Here the shape factor for peat given by Campbell et al. (1994) is used ($g_a = 0.33$). For a more detailed treatment of how shape factors are calculated, see de Vries (1963). Since Campbell et al. (1994) do not consider organic material separately from the minerals in the soil mixture, k_m is determined separately. The formula is essentially the same as the ones above with the only difference being a different shape factor g_m for the mineral constituent

$$k_m = \frac{1}{3} \left[\frac{2}{1 + \left(\frac{\lambda_m}{\lambda_f} - 1\right)g_m} + \frac{1}{1 + \left(\frac{\lambda_m}{\lambda_f} - 1\right)(1 - 2g_m)} \right].$$

The value of $g_m = 0.1$ is used to approximate the shape factors reported by Campbell et al. (1994) for the various mineral soils considered.

Proceeding toward an update rule for temperature, Equation (3) may now be discretized in a fashion similar to that of Equation (4). Expanding the right hand side

$$\nabla \cdot (K \nabla T) = \nabla K \cdot \nabla T + K \nabla^2 T = \frac{\partial K}{\partial x} \frac{\partial T}{\partial x} + \frac{\partial K}{\partial y} \frac{\partial T}{\partial y} + K \left(\frac{\partial^2 T}{\partial x^2} + \frac{\partial^2 T}{\partial y^2} \right).$$

Substituting the above into Equation (3),

$$C \frac{\partial T}{\partial t} = \frac{\partial K}{\partial x} \frac{\partial T}{\partial x} + \frac{\partial K}{\partial y} \frac{\partial T}{\partial y} + K \left(\frac{\partial^2 T}{\partial x^2} + \frac{\partial^2 T}{\partial y^2} \right) + \zeta H d_w \frac{\partial \theta}{\partial t} - \kappa_c C (T - T_a).$$

For the purposes of numerical stability and greatly increased computational speed, it is reasoned that $\frac{\partial K}{\partial x}$ and $\frac{\partial K}{\partial y}$ are zero. The purpose of the heat and moisture dynamics, roughly speaking, is to estimate the time it takes to make the transition from “wet” to “dry.” During this transition, the thermal conductivity can be expected to be on the same order as the initial thermal conductivity due to high moisture content away from the smoldering front. Once the moisture gradient becomes steep enough to significantly affect the spatial deriva-

tives of thermal conductivity, $\frac{\partial K}{\partial x}$ and $\frac{\partial K}{\partial y}$, the probability of consumption is already large. This reasoning is empirically verified since there appears to be no discernible difference in model behavior when these terms are dropped (with the exception that the truncated equation results in a faster scheme that appears to be stable). Therefore, the equation for heat transport is truncated to

$$C \frac{\partial T}{\partial t} = K \left(\frac{\partial^2 T}{\partial x^2} + \frac{\partial^2 T}{\partial y^2} \right) + \zeta H d_w \frac{\partial \theta}{\partial t} - \kappa_c C (T - T_a).$$

The above is then discretized using a forward difference in time and a centered difference in space,

$$\begin{aligned} C_t^{i,j} \frac{T_{t+1}^{i,j} - T_t^{i,j}}{\Delta t} &= K_t^{i,j} \left(\frac{T_t^{i+1,j} - 2T_t^{i,j} + T_t^{i-1,j}}{(\Delta x)^2} + \frac{T_t^{i,j+1} - 2T_t^{i,j} + T_t^{i,j-1}}{(\Delta y)^2} \right) \\ &+ \zeta d_w H_t^{i,j} \frac{\theta_{t+1}^{i,j} - \theta_t^{i,j}}{\Delta t} - \kappa_c C_t^{i,j} (T_t^{i,j} - T_a). \end{aligned}$$

Rearranging the above and simplifying, assuming $\Delta y = \Delta x$, the update rule for temperature in the non-smoldering regions ($\beta_{t+1}^{i,j} \neq 1$) is

$$\begin{aligned} T_{t+1}^{i,j} &= T_t^{i,j} + k_t^{i,j} [T_t^{i+1,j} + T_t^{i-1,j} + T_t^{i,j+1} + T_t^{i,j-1} - 4T_t^{i,j}] \\ &+ \frac{\zeta d_w H_t^{i,j}}{C_t^{i,j}} (\theta_{t+1}^{i,j} - \theta_t^{i,j}) - \kappa_c \Delta t (T_t^{i,j} - T_a) \\ &:= u_T(S_t^{i,j}, \theta_{t+1}^{i,j}) \end{aligned}$$

where, $k_t^{i,j} = \min \left\{ \frac{\Delta t K_t^{i,j}}{(\Delta x)^2 C_t^{i,j}}, k_{max} \right\}$. k_{max} is an upper bound on $k_t^{i,j}$. Limiting $k_t^{i,j}$ increases stability of the numerical scheme. A constant value of $k_t^{i,j}$ less than $k_{max} = 0.25$ guarantees stability for the uncoupled temperature dynamics (Haberman, 1998). Allowing $k_t^{i,j}$ to vary, a value of $k_{max} = 0.1$ appears to give reasonable predictive success and

stability when the moisture dynamics are included.

Temperature in the smoldering regions is determined in part by duff thickness $\tau^{i,j}$. Miyanishi (2001) and Miyanishi and Johnson (2002) note that duff depth plays a significant role in whether or not a smoldering front propagates. The smoldering boundary of a thin duff layer is more prone to losing thermal energy to convective heat loss, thermal energy that would otherwise be used to drive off moisture and sustain the combustion process. The model accounts for this phenomenon by scaling back the combustion temperature T_c at the smoldering front by an *efficiency* factor that depends upon the depth of the ignited cell. The efficiency factor approaches 1 as depth increases, indicating a maximum efficiency of the smoldering front to impart thermal energy to the soil. The efficiency factor is given by $\frac{1}{1+\varepsilon_1 e^{-\varepsilon_2 \tau^{i,j}}}$ where ε_1 and ε_2 are efficiency parameters.

The update rule for temperature is then

$$T_{t+1}^{i,j} = \begin{cases} u_T(S_t^{i,j}, \theta_{t+1}^{i,j}) & \text{if } \beta_{t+1}^{i,j} \neq 1 \\ (T_c - T_a) \left(\frac{1}{1+\varepsilon_1 e^{-\varepsilon_2 \tau_t^{i,j}}} \right) + T_a & \text{if } \beta_{t+1}^{i,j} = 1. \end{cases} \quad (8)$$

Implementation

Using the update rules developed in the above sections (Equations (5)-(8)), the model is implemented using code written in MATLAB[®].

RESULTS AND DISCUSSION

Overall Model Behavior

Spatial Patterns

One of the primary goals of this effort is to capture spatial patterns observed when duff undergoes smoldering combustion. Some of the more unusual patterns are observed when duff is at the limits of smoldering combustion. This transition occurs when the duff is either too moist or the inorganic content is too high. Since duff moisture is the only temporally variable duff characteristic on the time scale considered, the spatial patterns near the limits of smoldering combustion are induced by increasing duff moisture where all other parameters are set to field measurements.

For all simulations, duff conditions were uniformly initialized to the mean field conditions for bulk density and inorganic content for spruce/pine duff reported by Frandsen (1997). Unless otherwise noted, each model run used the regression coefficients for spruce/pine (*Pinus-Picea*) duff reported by Frandsen (1997).

The evolution of a typical simulated smoldering front initiated at the center of the lattice is seen in Figures 7, 8, and 9. The three model runs included both moist conditions near the limits of smoldering combustion (Figure 8, 105% GMC and Figure 9, 110% GMC) and dry conditions (Figure 7, 20% GMC). The first graph in each figure represents the initial combustion state (center ignition at $t = 0$) of each cell and each subsequent graph displays the combustion state 24 hours after the previous graph. In each figure of burn state versus space, unburned cells are colored blue, burning cells are colored green, and burned cells are colored red.

Model behavior when combustion is initiated at the left edge of the lattice is seen in

Figure 10 (20% GMC), Figure 11 (105% GMC), and Figure 12 (110% GMC). Figures 11 and 12 display how the model predicts the response of a smoldering front to moist conditions that no longer favor smoldering. Such conditions occur when there is a steep moisture gradient (such as at the drip line at the crown perimeter of a tree after a rain event).

The end stage of the smoldering process (when the process is allowed to proceed until all combustion ceases) is seen in Figures 13 and 14. Six consecutive simulations were run for moist soil conditions (105%, 110% GMC) using both initial burn configurations. Each simulation was allowed to proceed until all combustion ceased. In the field, a typical observation is unburned “islands” of soil (Miyaniishi and Johnson, 2002). Figures 15 and 16 show that the model predicts this phenomenon near the limits of smoldering combustion.

To understand how the simulated burned patch size varies near the limits of smoldering combustion, an empirical distribution representing 2400 simulations was generated (Figure 17). For each trial, ignition was initiated at the center of the lattice. The above serves as an example of how repeated simulation provides useful information concerning spatial aspects of duff consumption.

The Drying Front

In order to accurately model the spatial patterns observed in a smoldering ground fire, the phenomenon of a drying front in duff is a key aspect this model seeks to capture. Figure 18 displays the combustion state and the associated heat and moisture dynamics from the same model run. The graph of gravimetric moisture content illustrates that regions exposed to the smoldering front are significantly drier than unexposed regions (orange) as indicated by the cells colored green and light blue. In other words, the model indeed predicts a drying region ahead of the smoldering front.

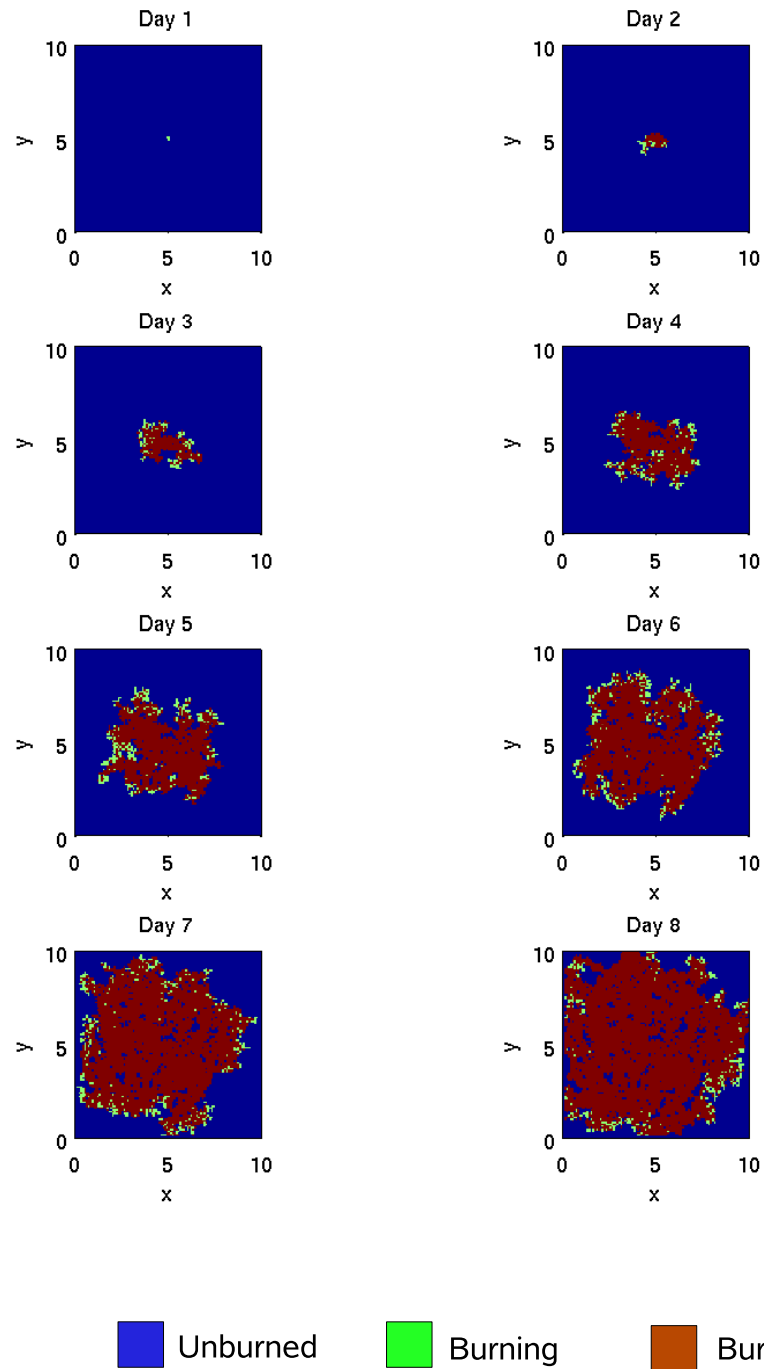


Figure 7: The evolution of a simulated smoldering front showing the spatial patterns that emerge for dry duff (20% GMC) with center ignition using regression coefficients for spruce/pine duff. $\mu_\gamma = 0.2$ kg/kg, $\mu_\rho = 116$ kg/m³, $\mu_\alpha = 0.307$ kg/kg, and $\mu_\tau = 0.15$ m.

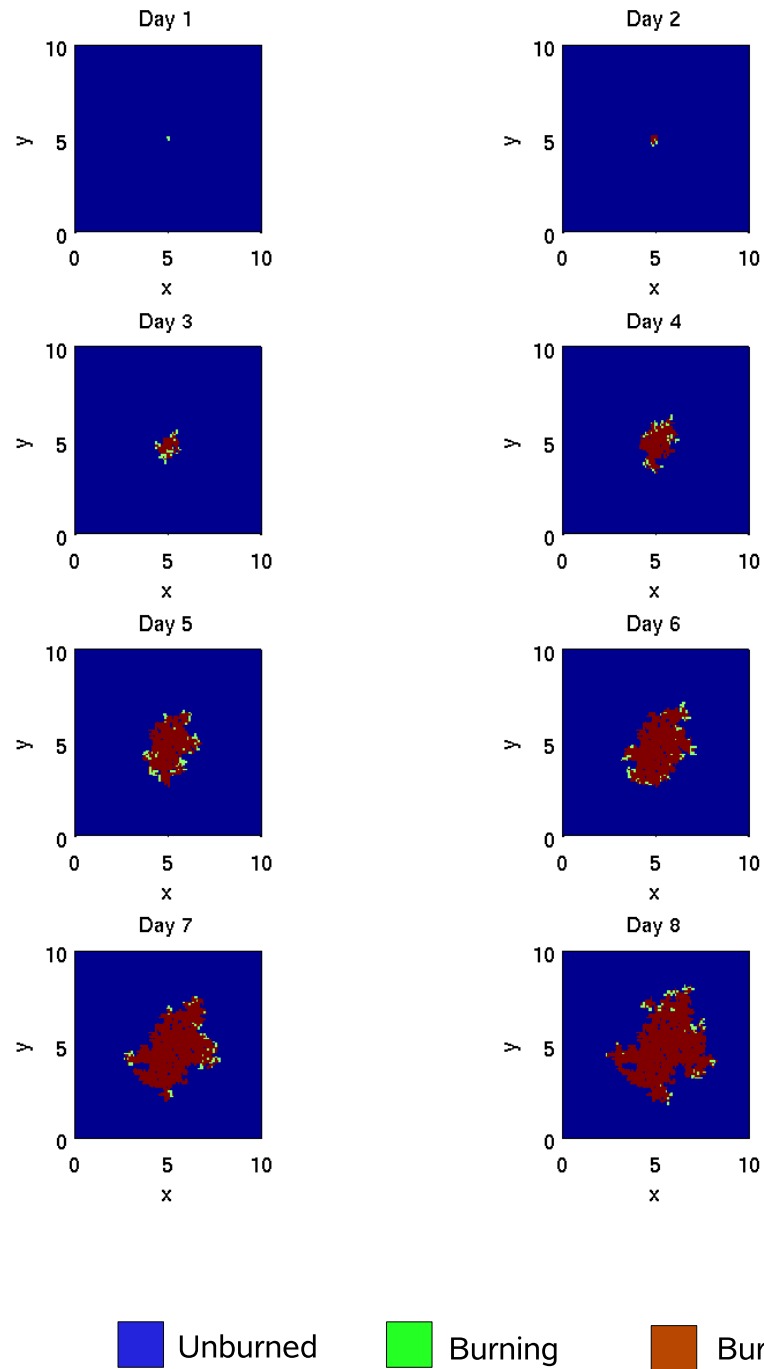


Figure 8: The evolution of a simulated smoldering front showing the spatial patterns that emerge for moist duff (105% GMC) with center ignition using regression coefficients for spruce/pine duff. $\mu_\gamma = 1.05 \text{ kg/kg}$, $\mu_\rho = 116 \text{ kg/m}^3$, $\mu_\alpha = 0.307 \text{ kg/kg}$, and $\mu_\tau = 0.15 \text{ m}$.

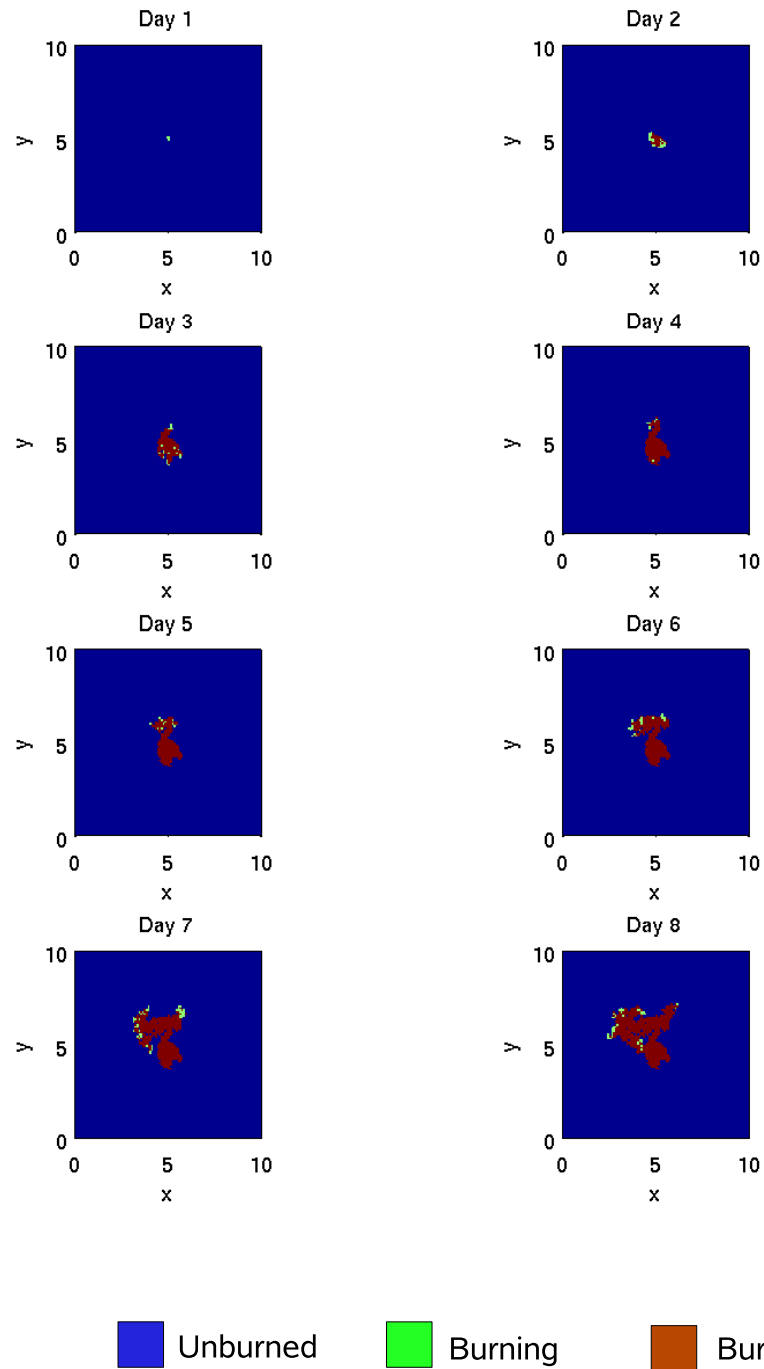


Figure 9: The evolution of a simulated smoldering front showing the spatial patterns that emerge for very moist duff (110% GMC) with center ignition using regression coefficients for spruce/pine duff. $\mu_\gamma = 1.1$ kg/kg, $\mu_\rho = 116$ kg/m³, $\mu_\alpha = 0.307$ kg/kg, and $\mu_\tau = 0.15$ m.

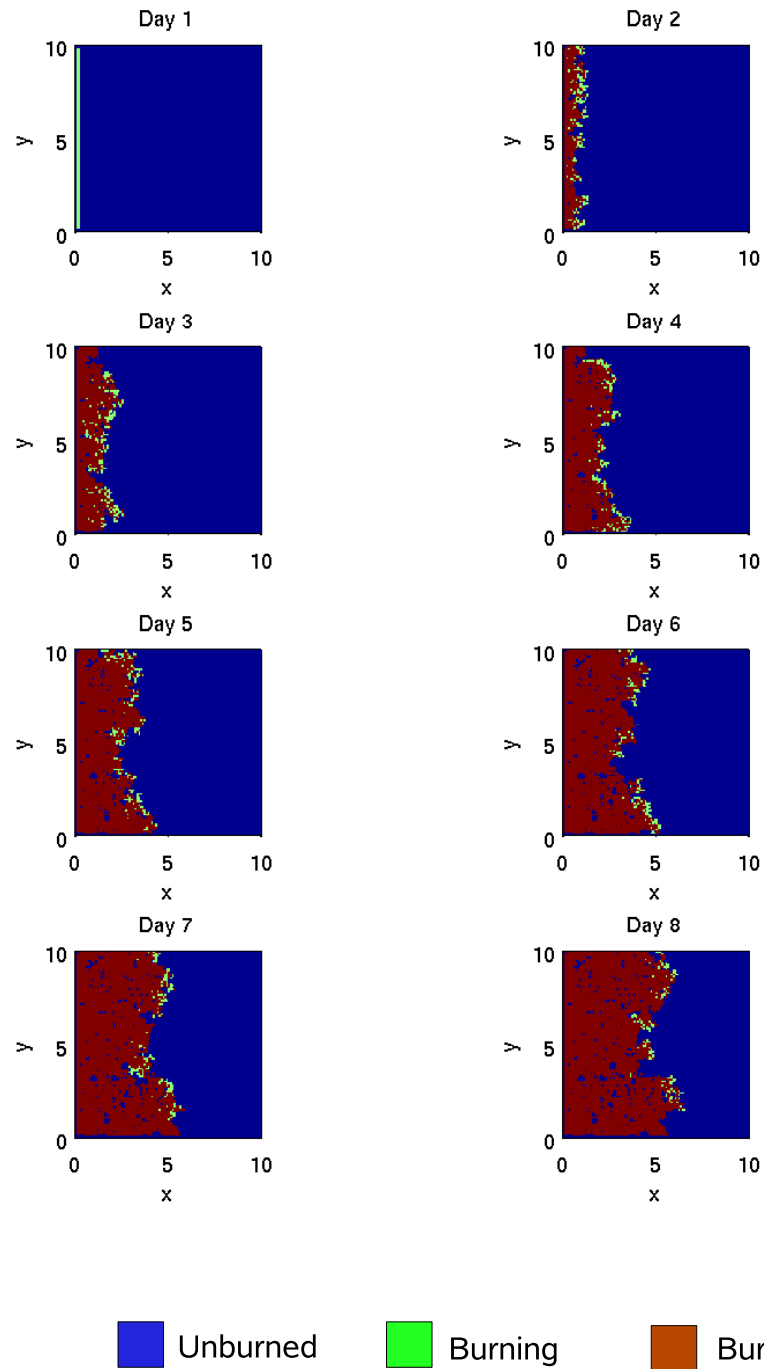


Figure 10: The evolution of a simulated smoldering front showing the spatial patterns that emerge for dry duff (20% GMC) with left edge ignition using regression coefficients for spruce/pine duff. $\mu_\gamma = 0.2 \text{ kg/kg}$, $\mu_\rho = 116 \text{ kg/m}^3$, $\mu_\alpha = 0.307 \text{ kg/kg}$, and $\mu_\tau = 0.15 \text{ m}$.

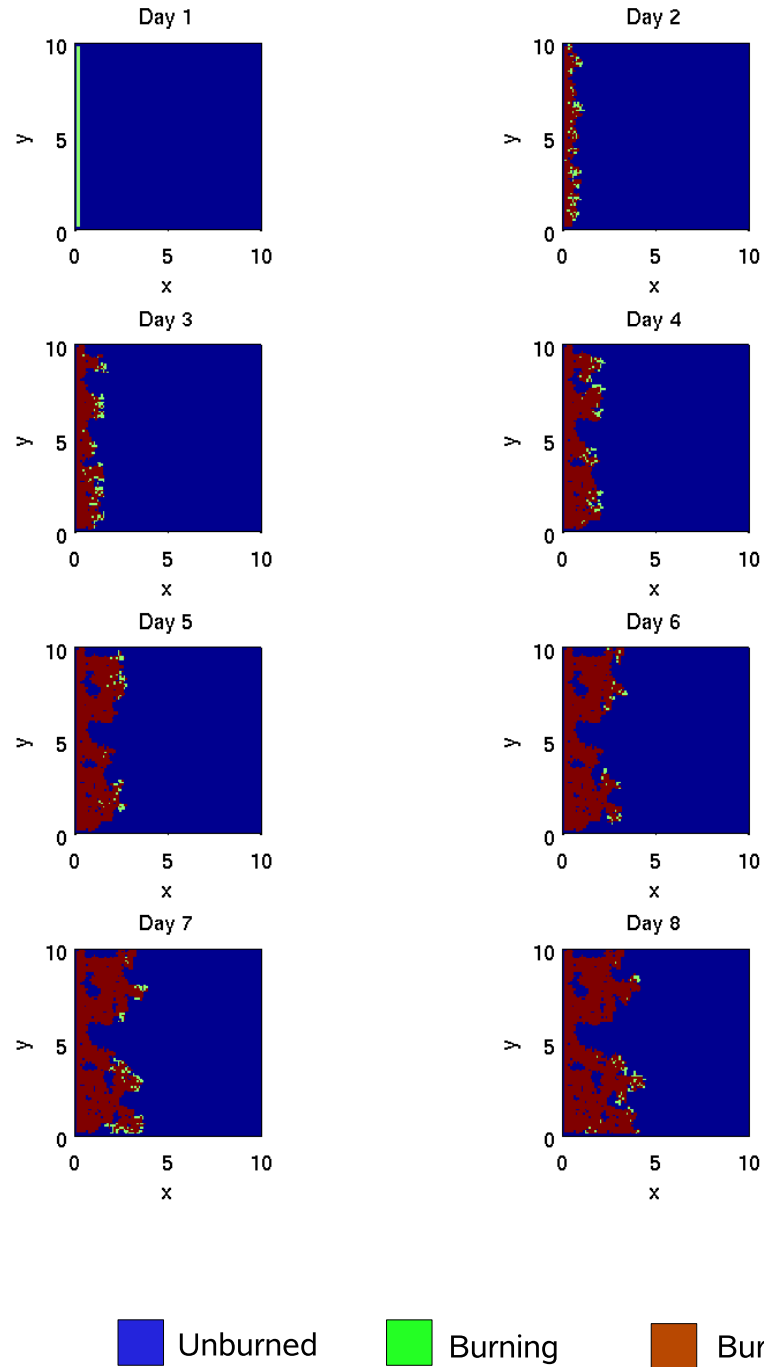


Figure 11: The evolution of a simulated smoldering front showing the spatial patterns that emerge for moist duff (105% GMC) with left edge ignition using regression coefficients for spruce/pine duff. $\mu_\gamma = 1.05 \text{ kg/kg}$, $\mu_\rho = 116 \text{ kg/m}^3$, $\mu_\alpha = 0.307 \text{ kg/kg}$, and $\mu_\tau = 0.15 \text{ m}$.

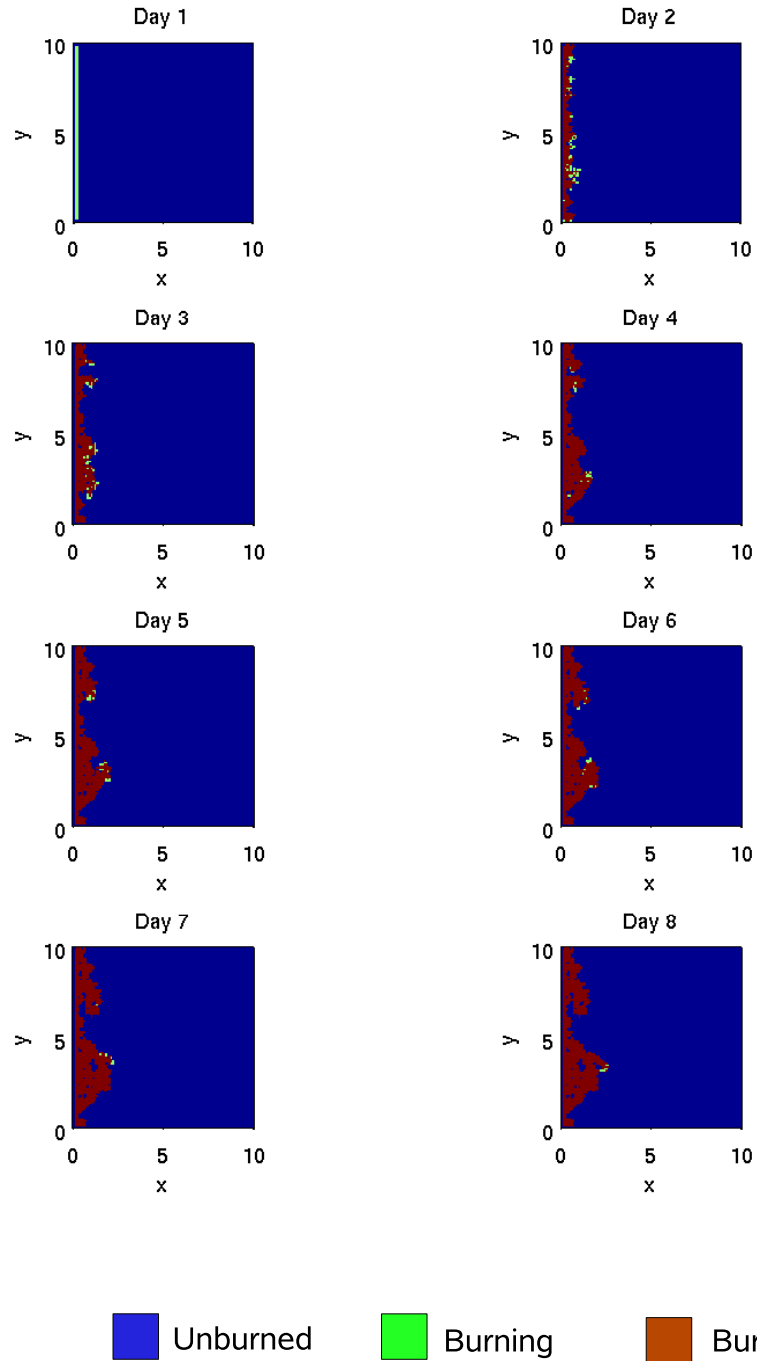


Figure 12: The evolution of a simulated smoldering front showing the spatial patterns that emerge for very moist duff (110% GMC) with left edge ignition using regression coefficients for spruce/pine duff. $\mu_\gamma = 1.1 \text{ kg/kg}$, $\mu_\rho = 116 \text{ kg/m}^3$, $\mu_\alpha = 0.307 \text{ kg/kg}$, and $\mu_\tau = 0.15 \text{ m}$.

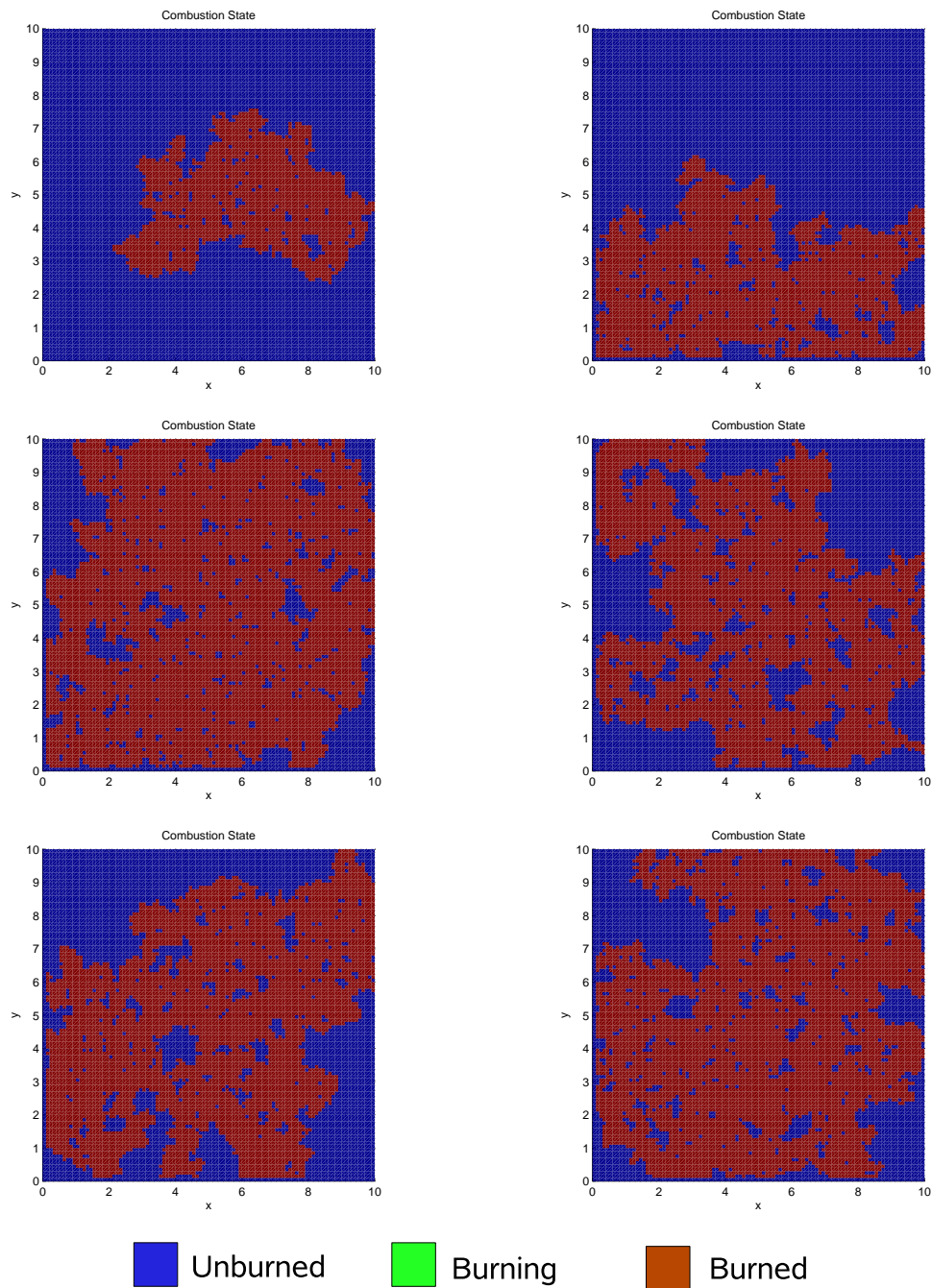


Figure 13: The resulting burn pattern for six consecutive model runs with moist duff (105% GMC) allowing the simulation to proceed until all combustion ceased. Ignition was initiated at the center. The initial uniform duff conditions were $\mu_\gamma = 1.05$ kg/kg, $\mu_\rho = 116$ kg/m³, $\mu_\alpha = 0.307$ kg/kg, and $\mu_\tau = 0.15$ m.

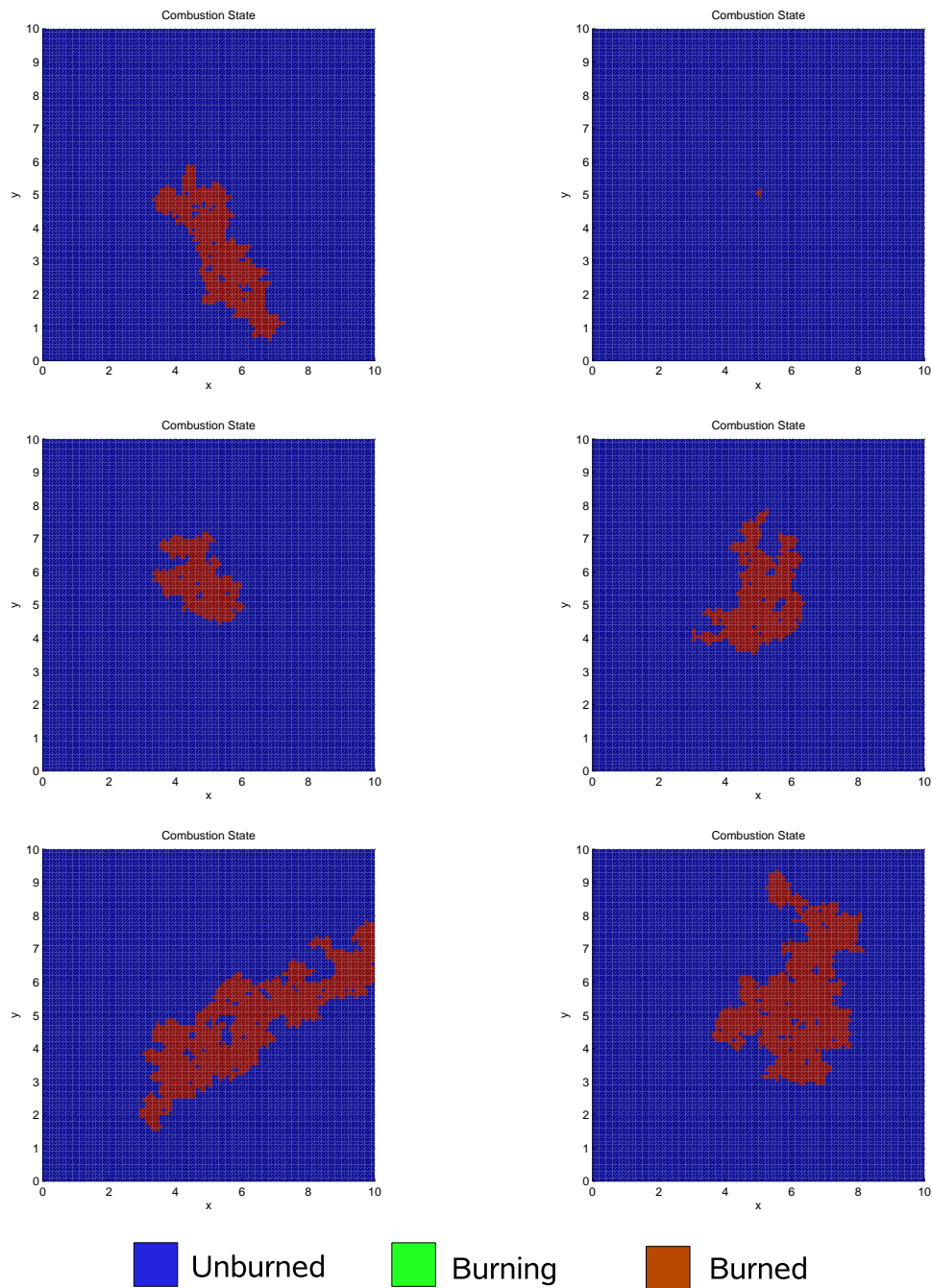


Figure 14: The resulting burn pattern for six consecutive model runs with very moist duff (110% GMC) allowing the simulation to proceed until all combustion ceased. Ignition was initiated in the center. The initial duff conditions were $\mu_\gamma = 1.1$ kg/kg, $\mu_\rho = 116$ kg/ m³, $\mu_\alpha = 0.307$ kg/kg, and $\mu_\tau = 0.15$ m.

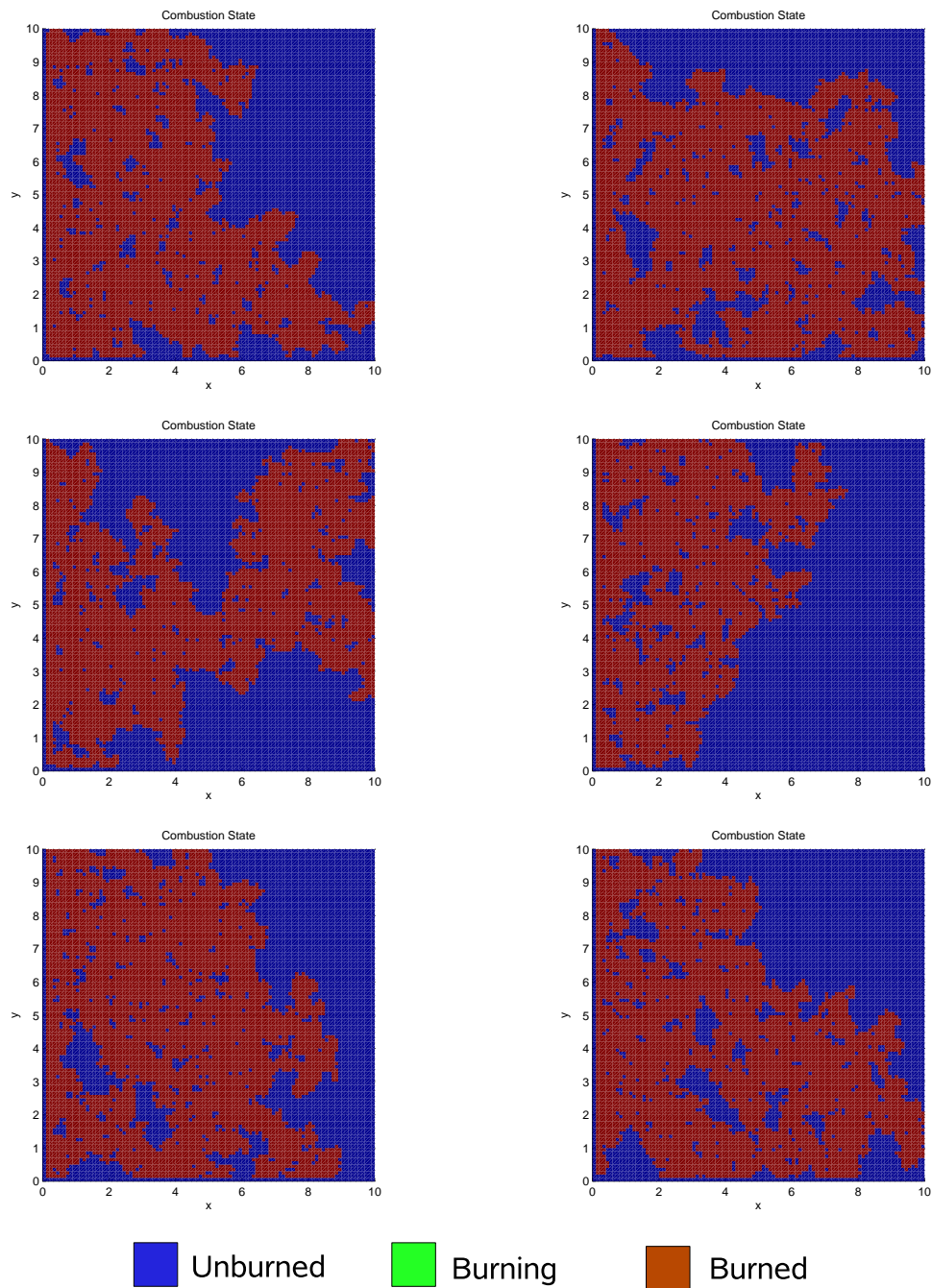


Figure 15: The resulting burn pattern for six consecutive model runs with moist duff allowing (105% GMC) the simulation to proceed until all combustion ceased. Ignition was initiated at the left edge. The initial duff conditions were $\mu_\gamma = 1.05$ kg/kg, $\mu_\rho = 116$ kg/m³, $\mu_\alpha = 0.307$ kg/kg, and $\mu_\tau = 0.15$ m.

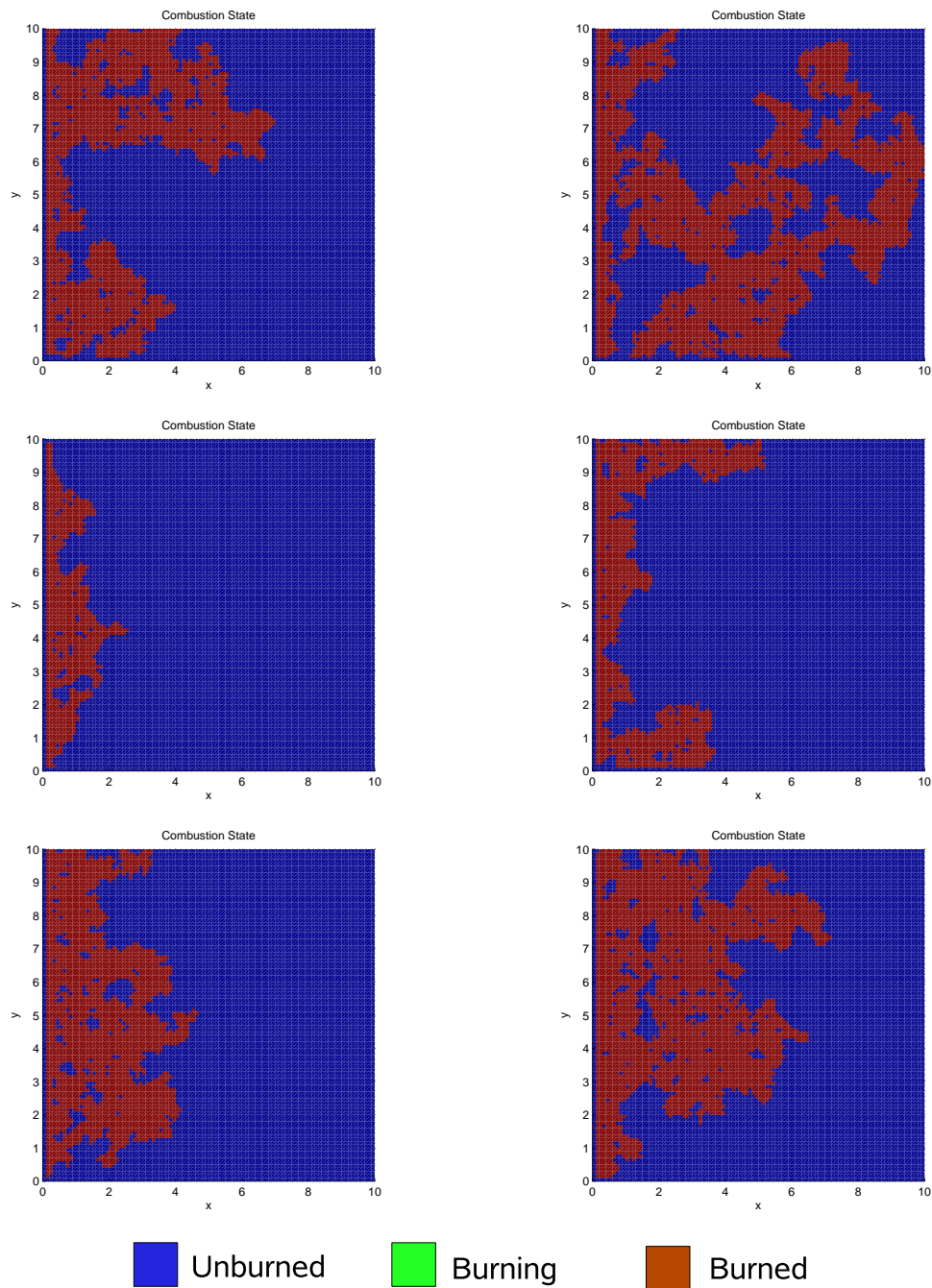


Figure 16: The resulting burn pattern for six consecutive model runs with very moist duff (110% GMC) allowing the simulation to proceed until all combustion ceased. Ignition was initiated at the left edge. The initial duff conditions were $\mu_\gamma = 1.1$ kg/kg, $\mu_\rho = 116$ kg/m³, $\mu_\alpha = 0.307$ kg/kg, and $\mu_\tau = 0.15$ m.

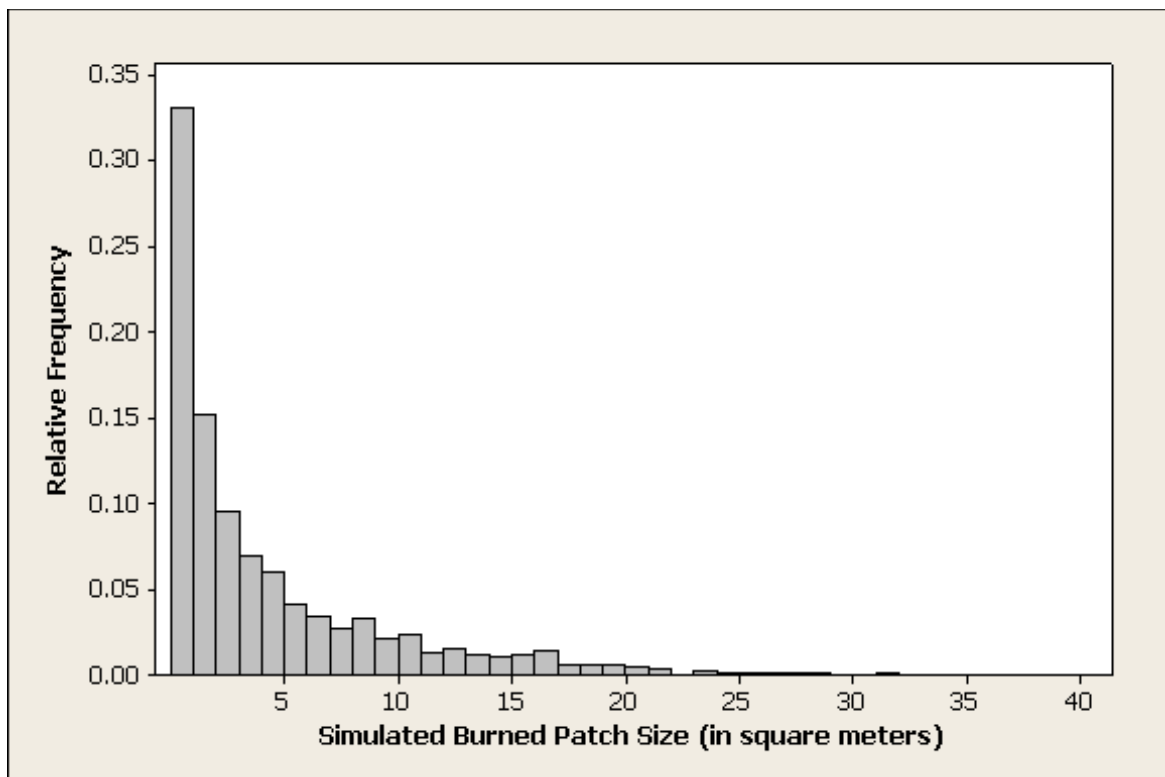


Figure 17: Histogram for the area (in square meters) of simulated burned patch sizes near the limits of smoldering combustion (very moist duff, 110% GMC) for 2400 trials with ignition initiated at the center of the lattice. $\mu_\gamma = 1.1$ kg/kg, $\mu_\rho = 116$ kg/m³, $\mu_\alpha = 0.307$ kg/kg, and $\mu_\tau = 0.15$ m.

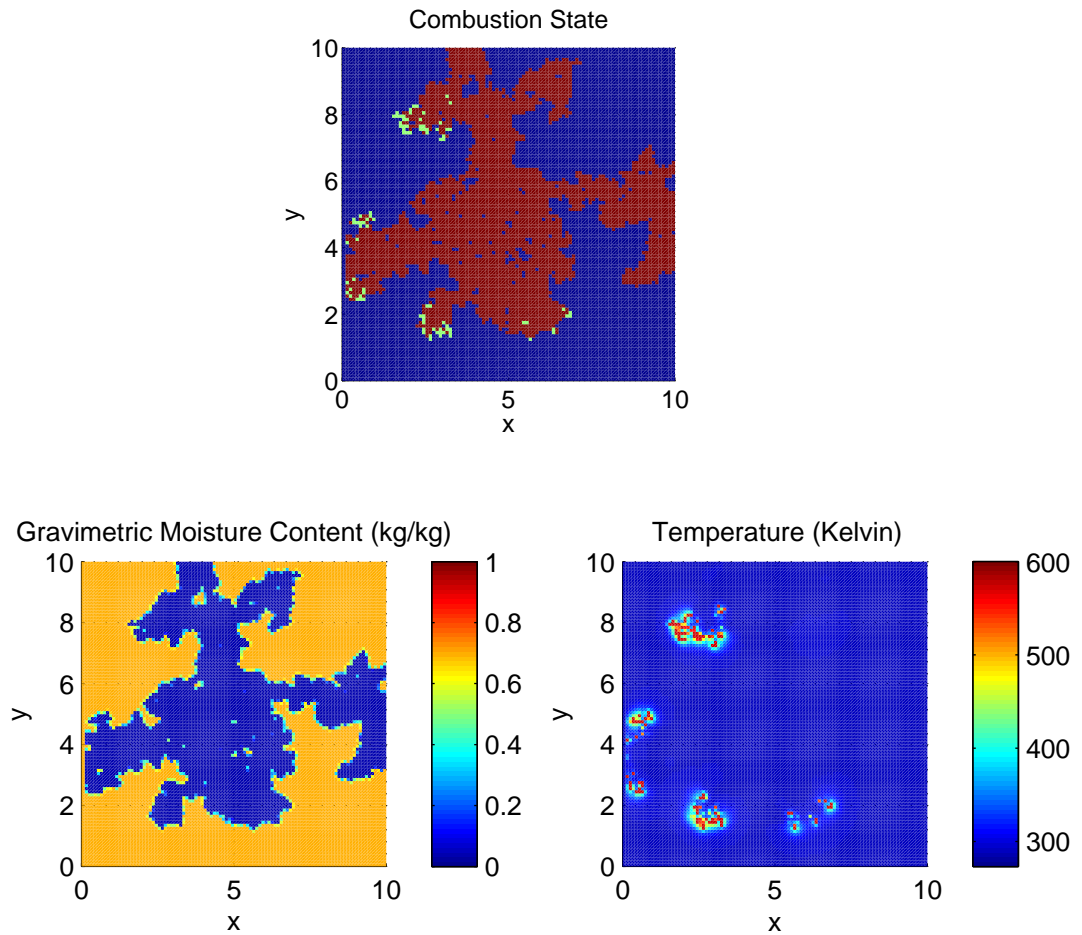


Figure 18: A model run in progress displaying also the heat and moisture dynamics. The predicted drying front is seen in the bottom left graph displaying moisture content versus space. $\mu_\gamma = 0.7 \text{ kg/kg}$, $\mu_\rho = 116 \text{ kg/m}^3$, $\mu_\alpha = 0.487 \text{ kg/kg}$, and $\mu_\tau = 0.15 \text{ m}$.



Figure 19: Smoldering duff in an aspen dominated stand during a prescribed burn. Ecosystem Management Emulating Natural Disturbance Project, Northwestern Alberta, Canada (photograph by David P. Shorthouse, University of Alberta, Bugwood.org).

Comparison of Model Behavior to Other Studies

Observed Spatial Patterns

Comparing a photograph of a typical burn pattern of a smoldering patch of duff (Figures 19 and 20) to a typical simulated burn pattern produced by the model (Figures 7-16) shows qualitative agreement.

The simulated temperature distribution (Figure 18) displays isolated patches of smoldering combustion indicating qualitative agreement with thermal images of actual smoldering ground fires (Figures 21 and 22).



Figure 20: Close up of smoldering duff with clearly defined smoldering boundary (photograph courtesy of J.M. Varner).

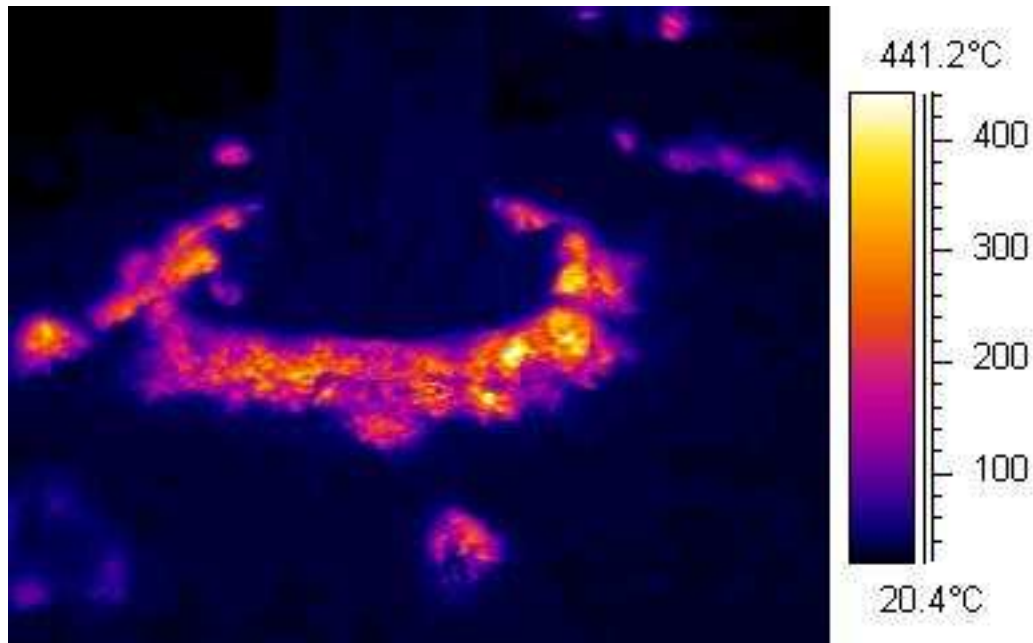


Figure 21: Thermal infrared image of duff smoldering at the base of a tree stem (image courtesy of J.M. Varner).

The Limits of Smoldering Combustion

In order to gain a sense of how the amount of duff consumed varies with the moisture and inorganic ratio (the ratio of the mass of water and inorganic solids to organic mass), the model was repeatedly run incrementing these parameters. For each run the initial simulated soil conditions were set to be uniform as in Frandsen (1987) and simulated bulk density for each run was the average field bulk density ($116 \frac{\text{kg}}{\text{m}^3}$) for spruce/pine duff reported by Frandsen (1997). The model was run for moisture ratios from 0 to 2 and inorganic ratios from 0 to 6, each in increments of 0.1 and the decimal percentage of duff consumed was recorded. The results of these simulations (Figure 23) are qualitatively similar to empirical results found in Frandsen (1987) in which peat samples with known uniform composition were exposed to an ignition source and a result of burn/no burn was recorded. Frandsen

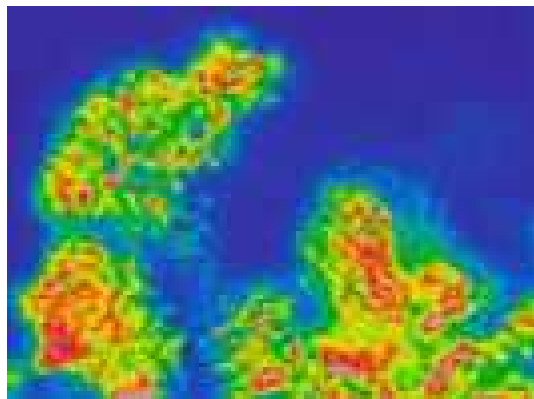


Figure 22: Mikron IR Camera image of smoldering duff (source: USFS-Missoula Montana Fire Science Lab).

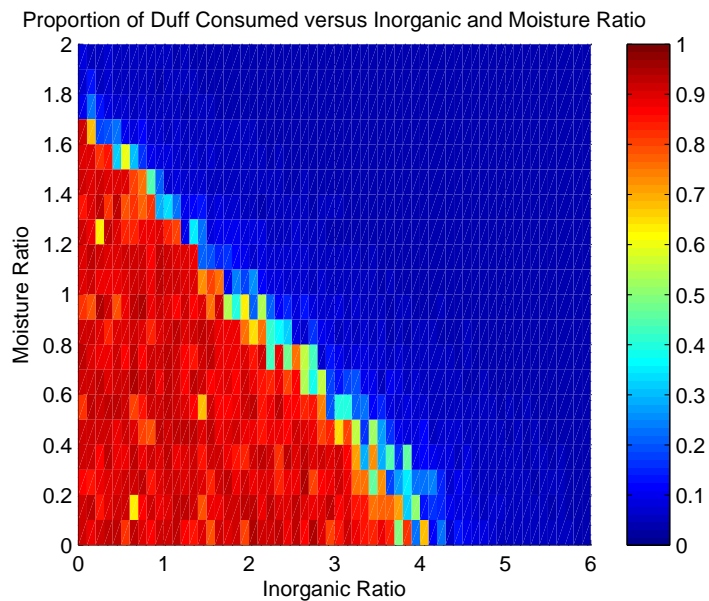


Figure 23: The proportion (denoted by color scale) of a simulated 10m by 10m patch of spruce/pine duff consumed by smoldering combustion expressed in terms of inorganic and moisture ratio. Each point represents the result of a single trial. $\mu_\rho = 116 \text{ kg/m}^3$, $\mu_\tau = 0.15 \text{ m}$.

observed that the line describing the limits of smoldering combustion for peat (the line separating the burn and no burn regions) has a vertical intercept of 1.1 and a horizontal intercept of 4. The model predicts a similar response in spruce/pine duff where the limits of smoldering combustion are described by a line with an approximate vertical intercept of 1.7 and an approximate horizontal intercept of 4 (Figure 23).

The same group of simulations was repeated using the regression coefficients given by Frandsen (1997) for white spruce (*Picea glauca*) duff. Again, the same pattern as above is observed (Figure 24). The model predicts that the limits of smoldering combustion for white spruce duff are described by a line with an approximate vertical intercept of 1.6 and an approximate horizontal intercept of 5.5. Each simulation used the mean field bulk density of $122 \frac{\text{kg}}{\text{m}^3}$ reported by Frandsen (1997).

The above results suggest that the line describing the limits of smoldering is a good characterization of the burn characteristics for a particular soil type.

Smolder Velocity

The simulated smolder velocity was measured using the same method described in the model formulation, with the exception that the duff conditions also determined the spread probability. Forty trials were conducted and then averaged to produce a predicted simulated smolder velocity at each combination of inorganic and moisture ratio. The simulated smolder velocity is compared to the smolder velocity of peat predicted by an empirical model by Frandsen (1991) that is based upon the mass consumption rate of peat (Figure 25). It is apparent that there is an overall qualitative agreement. However, the delayed effect of the inorganic ratio accounted for in Frandsen's model is not present in the lattice model; Frandsen's predicted smolder velocity is not affected by the inorganic ratio until it

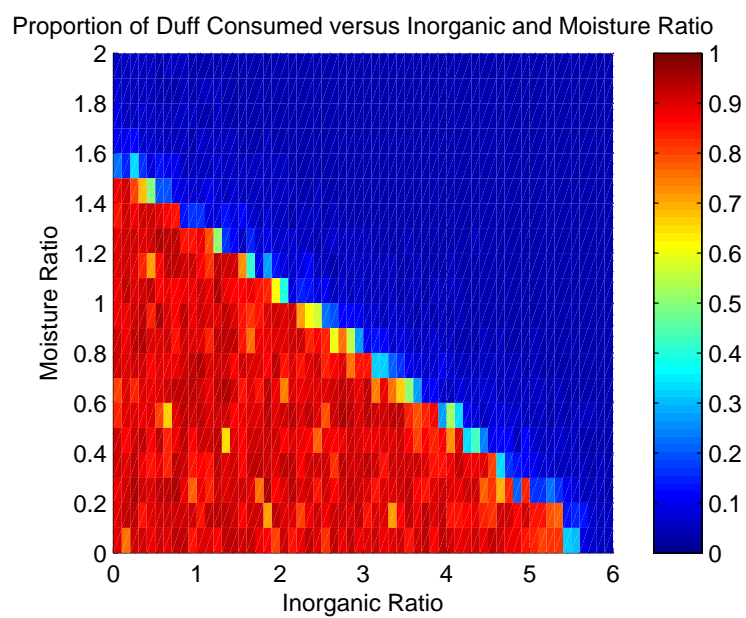


Figure 24: The proportion of a simulated 10m by 10m patch of white spruce duff consumed by smoldering combustion expressed in terms of inorganic and moisture ratio. Each point represents the result of a single trial. $\mu_\rho = 116 \text{ kg/m}^3$, $\mu_\tau = 0.15 \text{ m}$.

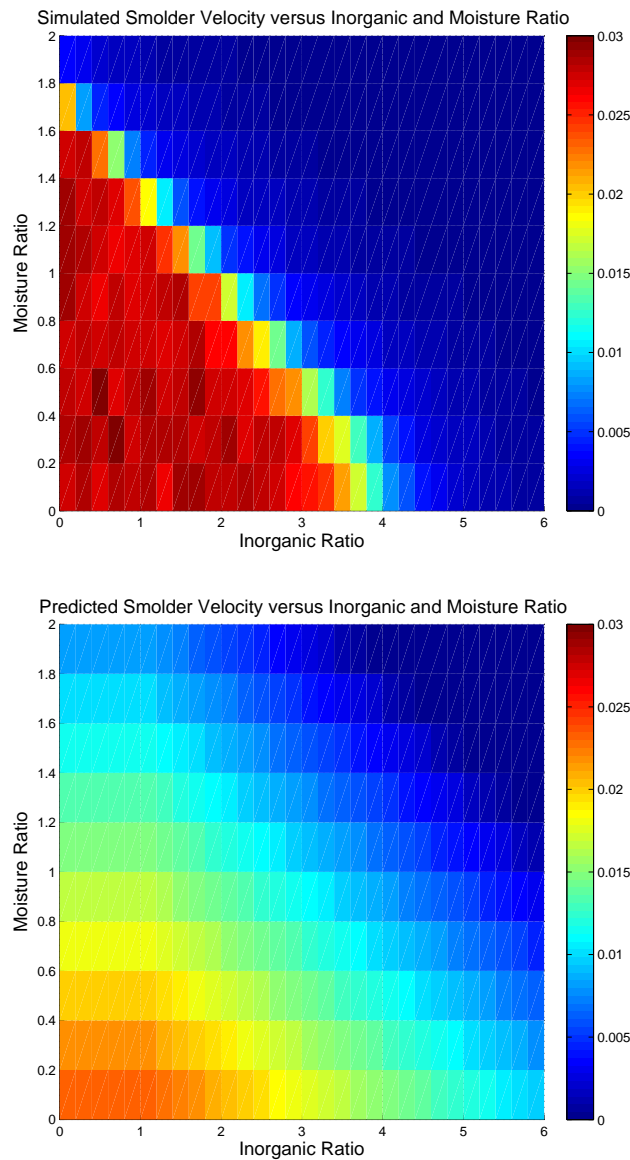


Figure 25: A comparison of simulated smolder velocities (top) for spruce/pine duff, $\mu_\rho = 116 \text{ kg/m}^3$, $\mu_\tau = 0.15 \text{ m}$, and smolder velocities predicted by the empirical model (bottom) of Frandsen (1991) for peat with the same bulk density. Each point of the simulated smolder velocity graph represents the average of forty trials.

reaches a value of 1. Also, the simulated smolder velocity does not appear to decrease until close to the limits of smoldering combustion where it then falls off rather sharply, whereas Frandsen's model predicts a linearly decreasing smolder velocity up to and past the limits of smoldering combustion. The sharp, sudden decrease in smolder velocity predicted by the lattice model is not unexpected, especially when comparing this behavior to how the moisture and organic ratio affect the amount of duff consumed (Figure 23). This decrease is in a global sense more in line with actual data than Frandsen's model since the data suggest that smolder velocities outside the region permitting smoldering combustion should be very close to zero. Also, Frandsen's model predicts a maximum smolder velocity of about $0.025 \frac{\text{m}}{\text{hr}}$, whereas, the maximum simulated smolder velocity is about $0.03 \frac{\text{m}}{\text{hr}}$.

The Effect of Depth

Although the model is two-dimensional, it accounts for the effect of depth (third-dimension) as well by means of the efficiency function describing efficiency versus depth that is included in Equation 8. The idea is that the smoldering perimeter more effectively transmits heat to the unconsumed soil due to less heat being carried off by convection (Miyanishi and Johnson, 2002). To test whether or not depth has any effect, the model was run for varying depth and volumetric moisture content and the average percentage duff consumed over five trials was recorded for each combination of these. The results (Figure 26) clearly demonstrate that depth does affect the behavior of the model. The results suggest that increasing depth allows for sustained combustion at higher moisture contents which is in line with empirical studies. One such study involving peat was performed by Miyanishi and Johnson (2002) in which an increasing trend of successful smoldering propagation with increasing depth is observed.

The pattern of successful ignition versus fuel depth and volumetric moisture content observed by Miyanishi and Johnson (2002) appears to resemble the overall pattern predicted by the model (Figure 26 and 27) when the proportion of duff consumed is interpreted as a measure of success of smoldering propagation. Simulated smoldering propagation could be considered “successful” if the proportion of duff consumed (which may be translated to an average linear distance traveled by the simulated front) exceeds some threshold. Letting this “success threshold” be 0.1 (an average smolder distance of 1 meter), the results (Figure 28) compare more favorably to the results of Miyanishi and Johnson (2002). However, with a higher success threshold, the two results do not compare as favorably in a quantitative sense, but an overall qualitative agreement is maintained. For both sets of simulations (Figures 27 and 28) the dry bulk density was $97 \frac{\text{kg}}{\text{m}^3}$ which is the same as the actual target dry bulk density used by Miyanishi and Johnson (2002). Differences between the simulated and observed results might be explained by other factors including fuel type. Modeling the influence of duff depth upon successful smoldering propagation is a matter that requires further investigation.

The extent to which the heat and moisture dynamics affect the overall behavior of the model is indirectly seen in Figures 26 and 27. With increasing depth, the efficiency with which the smoldering front imparts thermal energy to the unconsumed soil also increases (with a limiting value of 1, see Equation 8). Since the relationship between depth and efficiency is assumed to be a strictly increasing relationship, depth indirectly accounts for efficiency. Hence, at an efficiency (depth) near zero, the temperature has very little effect with little moisture being driven off ahead of the front. However, as the maximum efficiency is approached (deeper duff), the temperature takes effect and drives off more moisture ahead of the front so that more duff is consumed. Thus, temperature and moisture dynamics are worthy of consideration in any spatially explicit model of duff consumption.

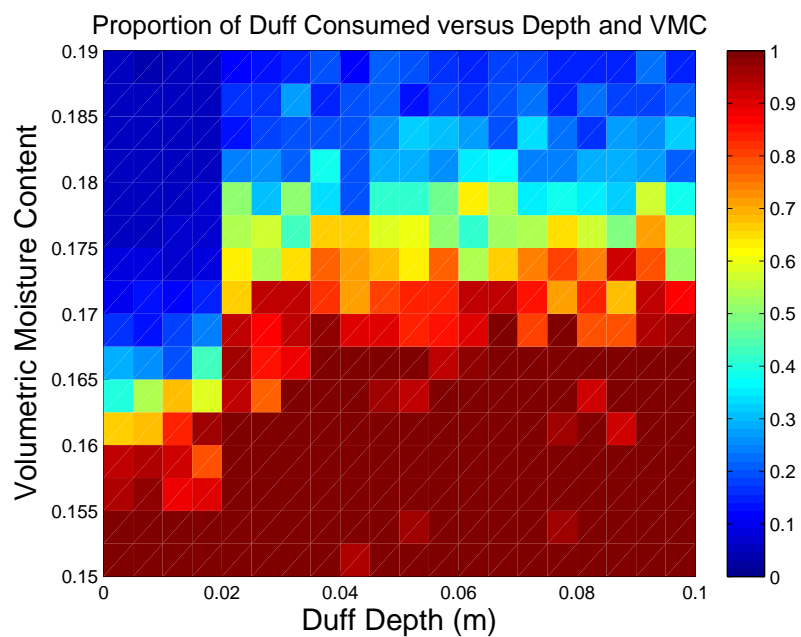


Figure 26: The percentage of a simulated 10m by 10m patch of spruce/pine duff consumed completely by smoldering combustion expressed in terms of depth and volumetric moisture content. Each point represents the average of five trials. $\mu_\rho = 116 \text{ kg/m}^3$, $\mu_\alpha = 0.307 \text{ kg/kg}$.

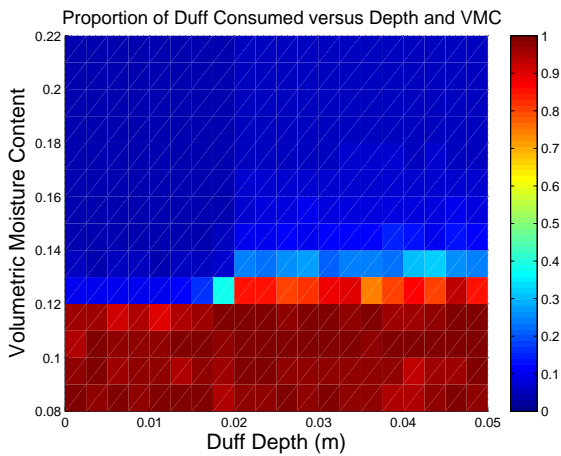


Figure 27: The percentage of a simulated 10m by 10m patch of spruce/pine duff consumed completely by smoldering combustion expressed in terms of depth and volumetric moisture content. Each point represents the average of five trials. $\mu_\rho = 67.2 \text{ kg/m}^3$ and $\mu_\alpha = 0.307 \text{ kg/kg}$ for a simulated dry bulk density of $\mu_\delta = 97 \text{ kg/m}^3$ used by Miyanishi and Johnson (2002).

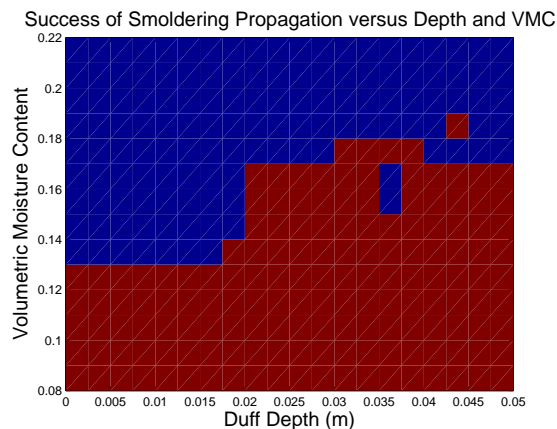


Figure 28: A plot of moisture-depth combinations that result in successful *simulated* smoldering propagation in spruce/pine duff where success is defined to be an average smolder distance greater than 1 meter. Red denotes successful propagation and blue represents failed propagation. Each moisture-depth combination represents 1 trial. $\mu_\rho = 67.2 \text{ kg/m}^3$ and $\mu_\alpha = 0.307 \text{ kg/kg}$ for a simulated dry bulk density of $\mu_\delta = 97 \text{ kg/m}^3$ used by Miyanishi and Johnson (2002).

MODIFICATIONS AND FUTURE WORK

Modeling the fuel bed as a lattice of cells offers multiple advantages. One advantage is that stochastic and deterministic models are easily coupled and integrated into the model. Another advantage is that better models (along with their numerical implementation) for the various phenomena considered (particularly, heat and moisture transport) are easily integrated into the model. Additionally, modifications are easily made to the model to answer other important questions concerning duff consumption.

By considering stand characteristics such as tree stem density, stem and crown diameters, and how duff depth and moisture varies in relation to these quantities (Hille and Stephens, 2005), an L by L meter area of forest may be simulated by stochastically initializing both the above quantities jointly with duff characteristics. Once a rule is established for how contact with smoldering duff influences whether or not a tree dies (by duration of and area of exposure, bark thickness, temperature of smoldering, etc.), a ground fire may be simulated (Figure 29) and an estimate of tree mortality caused by exposure to smoldering duff may be generated by repeated simulation.

The two-dimensional lattice of cells can also model a vertical cross section of duff rather than a horizontal layer as presented here (Figure 30). With minor modifications taking orientation and the heterogeneity of the various organic soil horizons into account, repeated simulation could predict duff depth reduction under a known set of conditions. Unlike the model representing a horizontal duff layer, the influence of the distinct structural differences between the duff horizons upon heat and mass transport could be explicitly accounted for. Repeated simulation of the model would not only offer mean and variance estimates of duff depth reduction, but would also predict a distribution for duff depth reduction. A one-dimensional lattice model of a soil column (Figure 30) might also

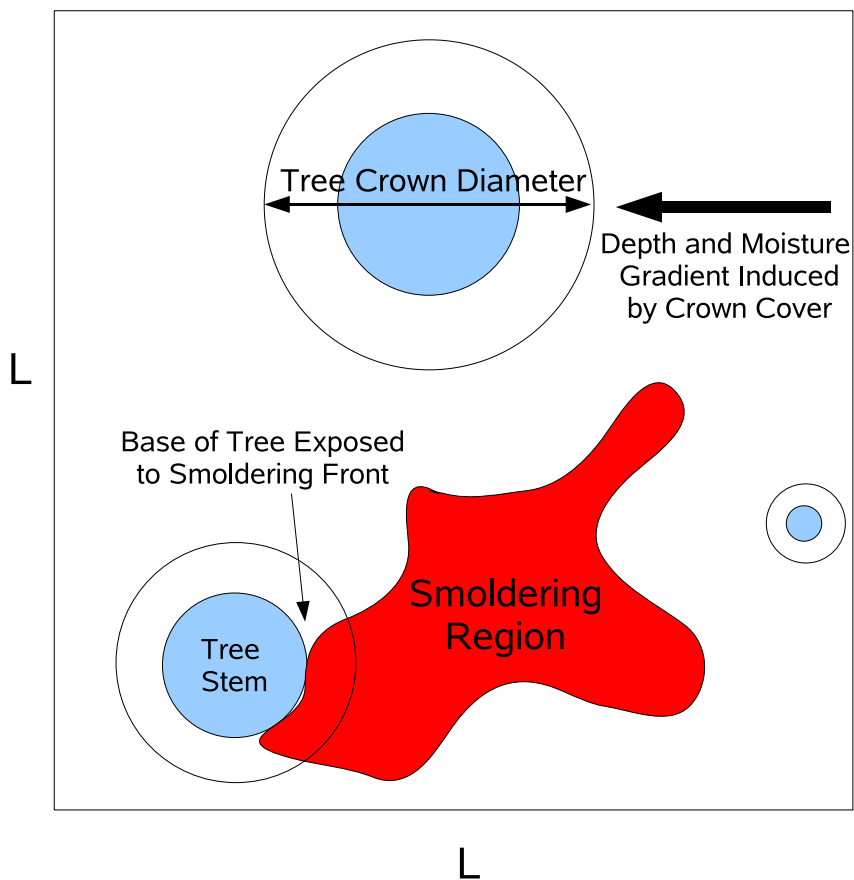


Figure 29: A modification to the model that includes stand structure to predict tree mortality. Stand characteristics and duff conditions would be stochastically initialized with duff characteristics varying jointly with crown cover and distance from stem. Repeated simulation would estimate of tree mortality caused by exposure to smoldering duff.

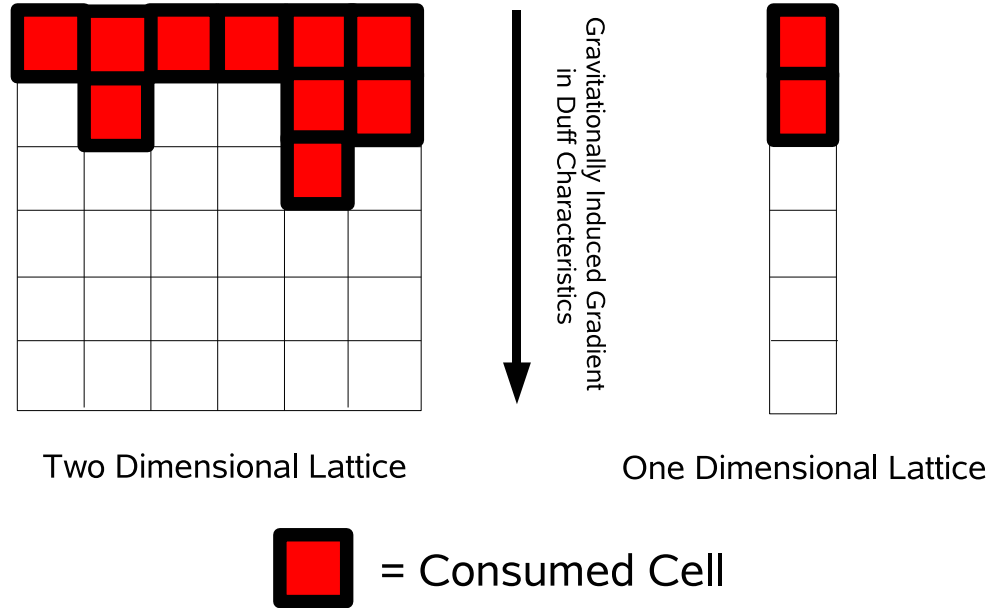


Figure 30: A modification to the model where the lattice of cells represents a vertical cross-section of duff instead of a horizontal layer. Repeated simulation would estimate duff depth reduction.

be considered. The numerical methods implementing heat and moisture dynamics would be more straight forward and computationally less intensive. It would also lend itself to one-dimensional models developed for soil columns (Campbell et al., 1995).

Duff depth reduction could also be estimated by introducing a slight modification to the model in which the depth of each cell decreases in a probabilistic fashion. Instead of duff depth remaining fixed in cells that are burning, depth would be allowed to vary according to some update rule. A prototype update rule is

$$\tau_{t+1}^{i,j} = \begin{cases} \max\{\tau_t^{i,j} - \Lambda_d \Delta t, 0\}, & \text{if } \beta_t^{i,j} = 1 \text{ and } U < \frac{1}{1+e^{-(B_0+B_1\mu_\gamma+B_2\alpha^{i,j}+B_3\rho^{i,j})}} \\ \tau_t^{i,j}, & \text{if } \beta_t^{i,j} \neq 1 \text{ or } U > \frac{1}{1+e^{-(B_0+B_1\mu_\gamma+B_2\alpha^{i,j}+B_3\rho^{i,j})}} \end{cases}$$

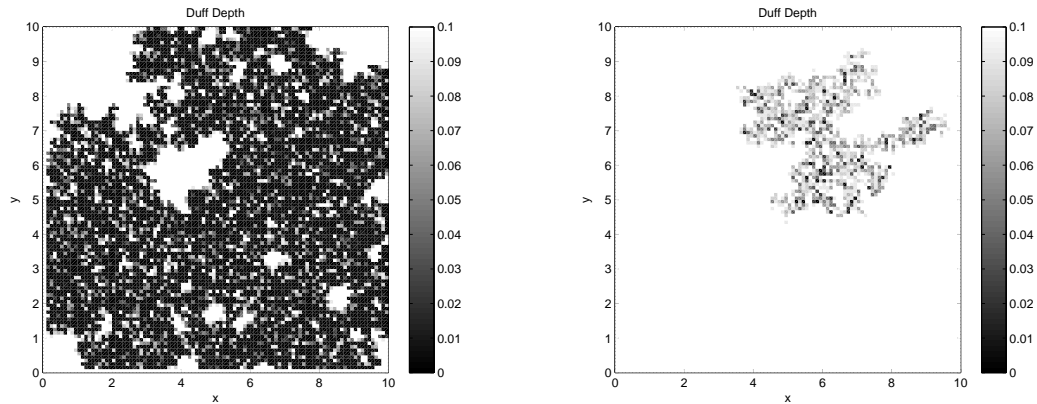


Figure 31: Output from the modified model after 8 simulated days where duff depth is allowed to decrease according to duff conditions. The graph on the left represents duff depth reduction for dry conditions (20% GMC) and the graph on the right represents duff depth reduction for very moist conditions (110% GMC). Both simulations used an initial uniform depth of 0.1 m with ignition initiated in the center. Regression coefficients for spruce/pine duff were used. $\Lambda_d = \Lambda = 0.05$.

where Λ_d is an uninhibited *downward* linear smolder velocity. Under ideal conditions, the depth smolders down to 0 with a smolder velocity of Λ_d . As duff conditions approach those that no longer favor smoldering, the “average” downward smolder velocity is scaled back by the probability statement of Frandsen (1997). Leaving all other update rules unchanged, the predicted depth reduction patterns of the modified model are promising (Figure 31), even with an update rule as simple as the one above. Improvements to this update rule might yield better results.

Three-dimensional cellular automata might also be considered in order to understand how ignition of the duff initiates a smoldering front in a three-dimensional volume of duff. A three-dimensional approach could directly account for mechanisms that drive duff consumption, such as the loss of thermal energy to convection at the burning surface. The deeper the duff layer, the less thermal energy lost to convective cooling (Miyaniishi and Johnson, 2002). The hypothetical three-dimensional model described above may offer

a more realistic efficiency function to use with Equation 8. A three-dimensional model would have the benefits of both the model developed here and its modification modeling a two-dimensional duff profile. However, the use of three-dimensional cellular automata is computationally intensive. The amount of time to run a single simulation would see a substantial increase (between one and two orders of magnitude), making repeated simulation less feasible. Additionally, the increased complexity of a three-dimensional model might not offer any more insight into the problems of duff depth reduction and tree mortality than separately using the two-dimensional modifications mentioned above.

It would also be interesting to consider how other neighborhood and lattice configurations affect model behavior. The model developed here updates the state of a given cell using information about itself and its four nearest neighbors. An update rule might also use the states of the eight nearest neighbors or cells lying within a certain distance (perhaps even using other metrics). Other lattice configurations might include slanted and hexagonal grid structures. Future efforts might consider how these different lattice configurations influence model behavior and the extent to which they approximate the various phenomena considered above.

Topography also influences duff depth and creates moisture gradients (Miyanishi and Johnson, 2002). Consequently, an improved model might also consider how topography influences variation in soil characteristics. Miyanishi and Johnson (2002) recommend that better hydrological models created specifically for duff be created. The model proposed here adds some urgency to this recommendation; such a result would be immediately useful in carrying out a modification to account for topographical features.

Under the assumption that soil characteristics are normally and independently distributed, stochastic initialization of the fuel-bed seems to have little effect on the qualitative behavior of the model. However, with better, more realistic initialization methods that take

into account the possible dependencies upon the various duff characteristics considered, differences in model behavior may become more apparent. A more formal investigation into how initialization (stochastic or otherwise) affects model behavior would be illuminating as a future course of study. Provided that site level variation has little effect on model behavior (Hillel (1998) indicates that in general bulk density and porosity have low site level variation), repeated simulations could yield information using only information about variation between L by L meter sites. For each run, uniform soil characteristics may be determined stochastically according to between-site distributions of these quantities. The above considerations suggest that any model of duff consumption attempting a broad, non-site-specific scope should also seek to understand within and between-site variation of duff characteristics. This model easily incorporates such information as it becomes available.

As mentioned above, heat and moisture dynamics do indeed have an effect upon the behavior of the model. The model predicts that with increasing depth (thermal efficiency), the percentage of duff consumed also increases. Consequently, further study and modifications to this work should include some treatment of heat and moisture dynamics. The effect of increasing consumption with increasing depth is validation of the model since Miyanishi and Johnson (2002) observe an increasing trend of complete consumption versus fuel depth. A three-dimensional cellular automaton model that directly accounts for mechanisms that drive thermal efficiency at the vertical smoldering surface (Miyanishi and Johnson, 2002) could provide a better efficiency function and offers one possibility for improving this aspect of the model.

Although there are general models for heat and moisture transport in soils, few, if any, specifically address these dynamics in *organic* soils. Efforts in this direction would almost certainly improve the performance of this model.

Models of heat and moisture dynamics in soils are generally non-linear and are con-

sequently difficult to solve numerically. Therefore other, more stable, numerical methods might be considered. Finite difference methods employed by the model can be unstable, and several assumptions had to be made to circumvent some of these difficulties. Although these simplifying assumptions are justified, a more robust numerical scheme might be developed. An appealing alternative to standard numerical procedures are recent methods, particularly those of Bandman (2002), developed for solving reaction-diffusion partial differential equations in a probabilistic fashion. The benefit of using stochastic methods is that they are unconditionally stable. Also, stochastic methods for describing heat and moisture transport are very much in line with the spirit of the work done here and would be an interesting modification to the model.

Suggested structural modifications to the model might reveal patterns that would otherwise be overlooked by empirical studies. Repeated simulations could provide empirical distributions for quantities such as patch size, duff depth reduction, and tree mortality resulting from smoldering duff. Empirical distributions for duff depth reduction and duff-induced tree mortality could be useful to prescribed burning and fire re-introduction (Ryan and Frandsen, 1991; Varner et al., 2007). Repeated simulation may also suggest patterns for how parameters for distributions change with changing conditions. An example of this is the decrease in the mean burned patch size with increasing moisture content. Empirical distributions may also suggest possibilities for exact distributions.

The model could also be useful in gauging the effects of prescribed burning to post-burn spatial heterogeneity. Fuel continuity caused by fire exclusion and the consequent lack of spatial heterogeneity in fuels and vegetation is favorable to some organisms, but detrimental to others, causing decline in biological diversity (Knapp and Keeley, 2006). Thus spatial heterogeneity, as measured by the variability and “patchiness” in ground cover, canopy cover, and other structural characteristics in the forest, is an important ecological

index of forest health. Low fuel loads believed to exist before fire exclusion are believed to have resulted in greater spatial heterogeneity in vegetation and fuels (Knapp and Keeley, 2006). Knapp and Keeley (2006) showed that it is possible to approximate the degree of spatial heterogeneity believed to exist before fire exclusion suggesting that computer models would be useful in predicting the degree of post-burn heterogeneity. Patch size distributions generated by the model developed here (Figure 17) offer measures of spatial heterogeneity in ground fuels. The duff consumption model developed here in conjunction with pair approximation techniques reviewed by Sato and Iwasa (2000) used to analyze spatial heterogeneity in lattice models may also prove to be a powerful combination in predicting and characterizing spatial heterogeneity in ground fuels.

Although this model is concerned with the combustion of organic forest soil, immediate application of the model and its modifications may be made to predict the behavior of peat fires which is a topic of growing concern since peat fires and the use of peat as fuel has been shown to have a large influence upon global carbon emissions. It is estimated that the peat fires of 1997 in Indonesia released between 0.19-0.23 billion tonnes of carbon into the atmosphere which is 13% to 40% of the annual mean global carbon emissions caused by fossil fuel consumption (Page et al., 2002). Page et al. (2002) notes that this event made a significant contribution to the largest recorded annual increase in the atmospheric concentration of carbon dioxide. A modified model may be used to estimate the impact that future peat fires could have on global carbon emissions.

CONCLUSIONS

Though there are many opportunities to improve the model and its implementation, this work has achieved the goals of creating a model of duff consumption that is easy to use, non-site-specific, and spatially and temporally accurate. The model predicts expected qualitative features concerning spatial patterns of duff consumption. The qualitative agreement with laboratory and field studies affirms that spatial patterns predicted by the model are indeed valid. A particularly appealing aspect of the model is that it is versatile. It is a general, non-site-specific model from which a site-specific model may be developed by considering a small number of easily measured, but key, parameters. The versatility of the model is not limited to its generality; the model is easily modified to account for other phenomena important to management practice and ecology, particularly, tree mortality and duff depth reduction. These potential models, when incorporated into models concerning other aspects of prescribed fires and wildfire, would be invaluable to helping foresters and ecologists in their efforts to restore biological diversity and overall forest health to fire suppressed regions.

BIBLIOGRAPHY

- Aston, A. R. and A. M. Gill. 1976. Coupled soil moisture, heat and water vapour transfer under simulated fire conditions. *Aust. J. Soil Res.*, **14**:55–66.
- Balland, V. and P. A. Arp. 2005. Modeling soil thermal conductivities over a wide range of conditions. *J. Environ. Eng. Sci.*, **4**:549–558.
- Bandman, O. 2002. Cellular-neural automaton: a hybrid model for reaction-diffusion simulation. *Future Generation Computer Systems*, **18**:737–745.
- Bradbury, A. G., Y. Sakai, and F. Shafizadeh. 1979. A kinetic model for the pyrolysis of cellulose. *J. Appl. Polymer Sci.*, **23**:3271–3280.
- Cahill, A. T. and M. B. Parlange. 1998. On water vapor transport in field soils. *Water Resources Research*, **34**:731–739.
- Campbell, G. S., J. D. Jungbauer, W. R. Bidlake, and R. D. Hungerford. 1994. Predicting the effect of temperature on soil thermal conductivity. *Soil Science*, **158**:307–313.
- Campbell, G. S., J. D. Jungbauer, K. L. Bristow, and R. D. Hungerford. 1995. Soil temperature and water content beneath a surface fire. *Soil Science*, **159**:363–374.
- Cosenza, P., R. Guerin, and A. Tabbagh. 2003. Relationship between thermal conductivity and water content of soil using numerical modeling. *Eur. J. Soil Sci.*, **54**:581–587.
- de Vries, D. A. 1958. Simultaneous transfer of heat and moisture in porous media. *Trans. Am. Geophys Union*, **39**:909–916.
- de Vries, D. A. 1963. Thermal properties of soils. In *Physics of Plant Environment*, pp. 210–235. North Holland Publishing Co., Amsterdam.
- Durrett, R. 1999. Stochastic spatial models. *SIAM Review*, **41**:677–718.
- Frandsen, W. H. 1987. The influence of moisture and mineral soil on the combustion limits of smoldering forest duff. *Can. J. For. Res.*, **17**:1540–1544.
- Frandsen, W. H. 1991. Burning rate of smoldering peat. *Northwest Science*, **65**:166–172.
- Frandsen, W. H. 1997. Ignition probability of organic soils. *Can. J. For. Res.*, **27**:1471–1477.
- Frandsen, W. H. 1998. Heat flow measurements from smoldering porous fuel. *Int. J. Wildland Fire*, **8**:137–145.

- Ghildyal, B. P. and R. P. Tripathi. 1987. *Soil Physics*. Wiley Eastern Limited, New Delhi, India.
- Haberman, R. 1998. *Elementary Applied Partial Differential Equations*. Prentice Hall, 3rd ed.
- Hille, M. and J. den Ouden. 2005. Fuel load, humus consumption and humus moisture dynamics in central european scots pine stands. *Int. J. Wildland Fire*, **14**:153–159.
- Hille, M. G. and S. L. Stephens. 2005. Mixed conifer forest duff consumption during prescribed fires: Tree crown impacts. *Forest Science*, **51**:417–424.
- Hillel, D. 1998. *Environmental Soil Physics*. Academic Press.
- Hiraiwa, Y. and T. Kasubuchi. 2000. Temperature dependence of thermal conductivity of soil over a wide range of temperature. *Eur. J. Soil Sci.*, **51**:211–218.
- Hungerford, R. D., W. H. Frandsen, and K. C. Ryan. 1996. Heat transfer into the duff and organic soil. Tech. Rep. FWS ref. no.14-48-0009-92-962 DCN 98210-2-3927, U.S Fish and Wildlife Service and U.S. Forest Service.
- Johansen, O. 1975. *Thermal Conductivity of Soils*. Ph.D. thesis, Norwegian Univ. of Science and Technol., Trondheim, Norway.
- Knapp, E. E. and J. E. Keeley. 2006. Heterogeneity in fire severity within early season and late season prescribed burns in a mixed-conifer forest. *Int. J. Wildland Fire*, **15**:37–45.
- McMahon, C. K., D. D. Wade, and S. N. Tsouklas. 1980. Combustion characteristics and emissions from burning organic soils. In *Proceedings of the 73rd Annual Meeting of the Air Pollution Control Association*. Montreal, Quebec. Paper No. 80-15.5.
- Miyanishi, K. 2001. Duff consumption. In *Forest Fires-Behavior and Ecological Effects*, pp. 437–474. Academic Press, San Diego, CA.
- Miyanishi, K. and E. A. Johnson. 2002. Process and patterns of duff consumption in the mixedwood boreal forest. *Can. J. For. Res.*, **32**:1285–1295.
- Naasz, R., J. C. Michel, and S. Charpentier. 2005. Measuring hysteretic hydraulic properties of peat and pine bark using a transient method. *Soil Sci. Soc. Am. J.*, **69**:13–22.
- Ochsner, T. E., R. Horton, and T. Ren. 2001. A new perspective on soil thermal properties. *Soil Sci. Soc. Am. J.*, **65**:1641–1647.
- Ohlemiller, T. J. 2002. *NFPA HFPE-02;SFPE Handbook of Fire Protection Engineering*, chap. 9, Smoldering Combustion, pp. 2/200–2/210. BFRL Publications, 3rd ed.

- Page, S. E., F. Siegert, J. O. Rieley, H. V. Boehm, A. Jaya, and S. Limin. 2002. The amount of carbon released from peat and forest fires in Indonesia during 1997. *Nature*, **420**:61–65.
- Ross, S. 2005. *A First Course in Probability*. Prentice Hall, 7th ed.
- Ryan, K. C. and W. H. Frandsen. 1991. Basal injury from smoldering fires in mature *Pinus ponderosa* Laws. *Int. J. Wildland Fire*, **1**:107–118.
- Sato, K. and Y. Iwasa. 2000. Pair approximations for lattice-based ecological models. In *The Geometry of Ecological Interactions: Simplifying Spatial Complexity*, pp. 341–358. Cambridge University Press.
- Steward, F. R., S. Peter, and J. B. Richon. 1990. A method for predicting the depth of lethal heat penetration into mineral soils exposed to various fire intensities. *Can. J. For. Res.*, **20**:919–926.
- Tarnawski, V. R., F. Gori, B. Wagner, and G. D. Buchan. 2000. Modeling approaches to predicting thermal conductivity of soils at high temperatures. *Int. J. Energy Res.*, **24**:403–423.
- van Genuchten. 1980. A closed-form equation for predicting the hydraulic conductivity of unsaturated soils. *Soil Sci. Soc. Am. J.*, **44**:892–898.
- Varner, J. M. 2005. Linking forest floor fuels with fire behavior and effects: A review of our knowledge and research. In *J. K. Hiers, D. R. Gordon, R. J. Mitchell, and J. J. O'Brien, Appendix B: Duff Consumption and Southern Pine Mortality (JFSP project 01-1-3-11)*, pp. 34–43. Joint Fire Science Program.
- Varner, J. M., D. R. Gordon, F. E. Putz, and J. K. Hiers. 2005. Restoring fire to long-unburned *Pinus palustris* ecosystems: Novel fire effects and consequences for long-unburned ecosystems. *Restoration Ecology*, **13**:536–544.
- Varner, J. M., J. K. Hiers, R. D. Ottmar, D. R. Gordon, F. E. Putz, and D. D. Wade. 2007. Overstory tree mortality resulting from reintroducing fire to long-unburned long leaf pine forests: the importance of duff moisture. *Can. J. For. Res.*, **37**. In press.